
Mini-Microscope based Optical Oxygen Sensor Development and Integration in an Automated Closed-Loop Organ on Chip Platform for Continual Oxygen Monitoring

By

NOEMI CALÁ



Master in Sistemi Elettronici, Ingegneria Elettronica
POLYTECHNIC UNIVERSITY OF TURIN

Defence Committee:

Prof Danilo Demarchi, Polytechnic University of Turin, Italy
Prof Yu Shrike Zhang, Brigham and Women Hospital, Har-
vard Medical School, Harvard-MIT Division of Health Sci-
ences and Technology, USA

JULY 2018

ABSTRACT

Oxygen is indispensable for cellular activities and is important to maintain it at the proper level which is different for each human organ.

Organ-on-a-chip systems are designed to simulate human tissue and organs. Their response are monitored by sensors, so that data can be measured in-situ and analyzed continuously in real-time.

In the field of drug research, most of the focus is in simulation and prediction of human organs response to external stress and requests due to drug delivery. Animal models are often not enough similar to human beings in order to obtain an accurate identification of the side effect of drugs in human. This is why the research is always more focused in the development of Organ-on-a-chip systems, where bio-mimetic organ models are integrated with biosensors in order to obtain accurate analysis of human organs dynamic responses to drugs.

This project describes the implementation of an automated closed-loop liver on chip system. The aim of the system is to provide a continuous oxygen control in organs on chips technology.

This thesis work is mostly focused on the design and development of a mini-microscope based optical oxygen sensor, moreover on the integration of the whole system and on the realization of an user interface.

The aim of the whole project is the development of a system constituted by an oxygen scavenger chip for decreasing oxygen concentration in cell culture media, that is the substance supporting the growth of cells, an oxygen generator chip for increasing oxygen concentration in cell culture media, a bioreactor to mimic human tissue, a peristaltic pump to control the culture media flow rate and mini-microscope-based oxygen optical sensor for real-time oxygen monitoring.

A MATLAB code is implemented in order to analyze the data obtained from the oxygen sensor.

The whole system is automatized and integrated using an Arduino board, controlling the mini-microscope-based oxygen sensor and the peristaltic pump. The oxygen optical sensor is developed by using a mini-microscope with an integrated dye indicator sensor, sensible to oxygen molecules. A blue LED is used as excitation source for the optical sensor and is turned on every time the culture media shall be sampled. The mini-microscope-based optical oxygen sensor receives command from Arduino in order to take samples each time slice, defined by the costumer, in order to have a continuous and automatized monitoring of the oxygen percentage in cell culture media. The sample are then analysed with a MATLAB code able to compute the culture media oxygen percentage by analysing the luminous intensity of the obtained pictures. The peristaltic pump receives commands from Arduino in order to control the scavenging solution flow rate related to the scavenger chip and, in this way, decrease the oxygen concentration of the culture media of the desired amount.

A graphical interface is developed, in order to provide a clear and easy to use interface to the costumers.

ACKNOWLEDGEMENTS

Firstly, I would like express my gratitude to my supervisor, Prof. Danilo Demarchi, who offered me this amazing experience at the Khademosheini Lab in Boston, MA. I would like to thank my laboratory supervisor, Yu Shrike Zhang, whose motivation and encouragement have been essential during these months. I need to thank my parents, my sister and my boyfriend, supporting me during my studies.

TABLE OF CONTENTS

	Page
List of Tables	vii
List of Figures	ix
1 Introduction	1
2 Aim of the project	5
3 Minimicroscope based Oxygen optical sensor	9
3.1 Introduction	9
3.2 Phosphorescence quenching oxygen sensor	10
3.3 Luminescence-based indicator and Detection of Luminescence intensity	14
3.4 Fabrication of optical oxygen sensor	14
3.5 MATLAB code for luminescence intensity analysis	18
3.6 Calibration Curve and Photobleaching correction curve	27
4 Oxygen Scavenger chip	30
4.1 Introduction	30
4.2 Scavenger chip design	32
4.3 Materials	33
4.4 Fabrication of Oxygen Scavenger chip	34
4.5 Scavenger test	40
5 Liver-on-chip Bioreactor	44

TABLE OF CONTENTS

5.1	Introduction	44
5.2	Bioreactor design and fabrication	45
5.3	Oxygen effect on liver on chips	48
6	Oxygen Generator chip	51
6.1	Introduction	51
6.2	Oxygen Generator chip design and fabrication	52
6.3	Generator test	54
7	Integration	56
7.1	Introduction	56
7.2	Integration and control	58
7.3	Peristaltic Pump control	59
7.4	RS485 interface	60
7.5	Connection schematic	62
7.6	MATLAB and Arduino code for integration	63
8	Conclusions	71
	Bibliography	74

LIST OF TABLES

TABLE	Page
2.1 The variations in physiological oxygen levels for different human tissues.	5
7.1 RTU Message Frame	61

LIST OF FIGURES

FIGURE	Page
2.1 Schematic setups for closed-loop liver on chip platforms with different oxygen levels.	7
3.1 Jablonski diagram showing the phosphorescence quenching by O ₂ process	12
3.2 Schematic and photograph of a custom made oxygen sensor.	15
3.3 Schematic and photograph of the custom made minimicroscope-based oxygen sensor.	16
3.4 RGB configuration of the CMSO sensor for the minimicroscope and analysis of the separate R/G/B channels.	17
3.5 Example of ruthenium beads image from minimicroscope.	18
3.6 3-D array of RGB triplets illustration.	20
3.7 Example of base image.	21
3.8 Example of mask image.	22
3.9 Example of mask image for dye beads selection.	23
3.10 Example of cropped bead areas image.	24
3.11 Oxygen sensor calibration curve.	28
3.12 Photobleaching correction curve.	29
4.1 Optimization of CO ₂ laser radiation fluence and beam speed for ablating plastic matrix (nominal thickness=3.0 mm). (a) Depth of the ablated regions as the laser beam fluence varied at a constant beam speed (0.76 mm s ⁻¹) and Z-axis (8.0 mm); (b) Depth of the ablated region as the laser speed was varied at a constant fluence (249 mJ mm ⁻²) and Z-axis (8.0 mm); (c) Depth of the ablated regions as the Z-axis varied at a constant fluence (249 mJ mm ⁻²) and beam speed (0.76 mm s ⁻¹) (n=3).	35

4.2	Photographs of laser ablated cross-sections of plastic matrix.	36
4.3	Optical and SEM images of laser engraved microchannels (a) and (b) before and (c) and (d) after chloroform treatment.	37
4.4	PDMS membrane thickness graph with respect to spin-coating rate	38
4.5	Modules for oxygen scavenging control. (a) Structure of oxygen scavenger which is consisted of three layers: two microfluidic PMMA layers and a sandwiched PDMS membrane. (b) Photographs of oxygen scavenger: top view and side view. Scale bar=1.5 cm.	39
4.6	Chaotic mixer. Scale bar = 1 cm	40
4.7	Scheme of the oxygen scavenger connected to the minimicroscope.	41
4.8	Outlet oxygen concentration as a function of flow rate within the bottom microfluidics with the Na_2SO_3 concentrations varying from 2 wt%-20 wt%.	42
4.9	Stability of the oxygen scavenger with a prolonged time of 180 min.	43
5.1	Schematic of liver-on-a-chip bioreactor where the patterned 3D encapsulated liver cells were entrapped within the bottom PMMA layer and covered with a top PMMA layer. An elastic PDMS membrane was sandwiched between PMMA layers for sealing.	46
5.2	Photographs of (i) photomask for patterning, (ii) top view and (iii) side view of bioreactor, and a micropillar of 3D encapsulated cells.	47
5.3	Oxygen uptake rate for $4 \cdot 10^6$ cells/ mL (70.000 cells in the hepatic construct) at different inlet flow rates. Scale bar = $mol\ m^{-3}$. Scale = 1 mm.	48
5.4	Cell metabolic activities as a function of different oxygen level. Scale bar= $200\ \mu m$	49
5.5	Oxygen consumption for 3D cell culture.	50
6.1	Schematic and photographs of oxygen generator: top view and side view. Food dye solution within the microchannels was used to demonstrate fluid flow. The magnified photograph shows a section of microfluidic patterns. Scale bar=1.5 cm. Inset scale bar=1.5 mm.	54
6.2	Measured oxygen level at both inlet and outlet.	55
6.3	Stability of the oxygen generator with a prolonged time of 180 min.	55

7.1	Layout of the Close-Loop Oxygen Control System.	57
7.2	MODBUS protocol.	62
7.3	MAX485 connection diagram.	62

INTRODUCTION

The drug discovery is a very long process, expensive and with high rate of failure. Failure of drug in human patients is mostly due to the inadequate animal models to properly establish the side effects and toxicity of drugs in human beings. It is necessary, therefore, to develop predictive platforms able to simulate the most important biological and physiological parameters of human organs and tissues. Different organ models can be connected using the microfluidics in a similar way to the reality. This leads to the possibility of having a more accurate prediction of human response and multiorgan interaction.

It is important to focus on the biosensing integration as well as the development of biomimetic organ models. The continuous *in situ* measurement, in fact, is essential to accurately evaluate organs parameters and dynamic responses to pharmaceutical compounds.

Some drugs can trigger chronic cellular reactions, other drugs can lead to delayed cellular responses. An integrated system combining perfectly organ models, microfluidics units and biosensors, working continuously and automatically for long time, would be the solution for drug validation processes.

The organ-on-chip systems emerged as solid platform for drugs validation. By using these systems it will be possible to substitute the traditional cell cultures, static, and eliminate the difference between animal models and human body. This means more reliable predictions of drugs safety

and efficacy in human beings with respect to previous methods.

Organ on chip microsystems are typically perfused with common culture media. Cell culture media is the nutritious compound that supports the growth of cells. Variations in culture media physical-chemical features can lead to undesired changes in organ models resulting in a degradation on prediction accuracy of the system for pharmaceutical screening.

Oxygen concentration is essential in cellular activities. An insufficient oxygen intake can cause variation in cellular metabolism and physiological pathways. On the other hand, high oxygen concentration can cause damages to cellular components.

The level of oxygen concentration is helpful in diagnosis formulation. Tissue hypoxia in cancerous tumors is associated to resistance to radiation therapy, to antitumour drugs, to the increased probability of metastasis and to a decreased probability of survival of the patient. Oxygen levels in cancers are generally lower than in healthy tissues.

Moreover, oxygen level is identified to be a very relevant parameter in stem cell differentiation and cultivation. The proliferation of stem cells can be improved in culture condition characterized by oxygen level below the typical 20%. Changing the oxygen concentration in stem cell culture surrounding can be useful as simulation of effects of the illness.

Oxygen concentration monitoring is fundamental for multi-organ-on-chip systems, where different organs need different oxygen concentration dissolved in culture media.

Different microfluidics optical techniques are developed in order to measure the oxygen in culture media. The optical oxygen measurement is principally based on alterations of optical property of oxygen markers detection. While changing the oxygen concentration, the fluorescent intensity of a marker is being monitored. Optical sensor performances are not affected by culture media flow rate and this is useful for microfluidics applications. The optical sensor can execute coherent and accurate measures in which a variable gamma of culture media flow rate is required.

Here, a mini-microscope imager with a built-in fluorescence oxygen sensor is developed and embedded with a microfluidic bioreactor in order to be used for monitoring the oxygen level dissolved in the culture media. This is integrated with an oxygen scavenger chip, oxygen generator chip and a bioreactor chip.

Each chip is developed, produced and tested in laboratory to ensure the correctness of the system

behaviour.

This thesis project is mostly focused on the design and development of a mini-microscope based optical oxygen sensor and on the integration of the whole system. In order to give a clearer view of the overall project and of the aim of this thesis project, all the different sections of the system are described in this text.

AIM OF THE PROJECT

The aim of the project is the development of a closed loop system capable of controlling the oxygen concentration of culture media in its different sections.

Each section of the system will be described in detail in the following chapters. Here an explanation of the overall project.

The start point is a culture media solution exposed to the atmosphere, which has an oxygen level of about 21%. Typically, the physiological oxygen levels in tissues and cells are below this amount. Under normal conditions, the oxygen level is about 3% in venous blood, 10-13% in arterial blood and in liver.

Organ	Oxygen level (%)
Lung alveoli	13-14
Venous blood	3-5
Muscle	2.7-4
Liver	10-13
Arterial blood	10-13
Bone marrow	0.5-7

Table 2.1: The variations in physiological oxygen levels for different human tissues.

This means that we need to decrease the oxygen concentration of the culture media before it reach the bioreactor.

The oxygen concentration decrease can be obtained by using the *oxygen scavenger chip* . The culture media is passed through the oxygen scavenger chip, where the oxygen concentration can be reduced from 21% to less than 10%. The outlet of the *oxygen scavenger chip* is then analysed by using the mini-microscope-based optical sensor that continuously monitor its correct functionality. Monitoring the *oxygen scavenger chip* outlet is very important, since it is connected to the inlet of the bioreactor: it is essential to ensure the proper amount of oxygen to the cells in order to do not interfere with their welfare.

Inside the bioreactor, cells perform an oxygen consumption due to their vital functions. At the outlet of the bioreactor we, therefore, expect a lower oxygen concentration of the culture media, that depends on the cell density of the bioreactor. Or better, by knowing the cell density of the bioreactor, the oxygen concentration of the culture media at its outlet depends on the amount of alive cells among the total. The outlet of the bioreactor is, again, analysed by a second mini-microscope-based optical oxygen sensor. In this way it is possible to evaluate the toxicity of the examined drug. If the oxygen concentration is not decreasing or not as expected, the drugs are probably having negative effects on cells.

Since it is a closed loop system, the oxygen concentration of the culture media at the outlet of the bioreactor needs to be increased, in order to be sent back to the *oxygen scavenger chip*. For this reason, the culture media is passed through the *oxygen generator chip*, able to increase the oxygen level from 10% to 21%. The schematic and picture of the whole developed system is shown in Figure 2.1.

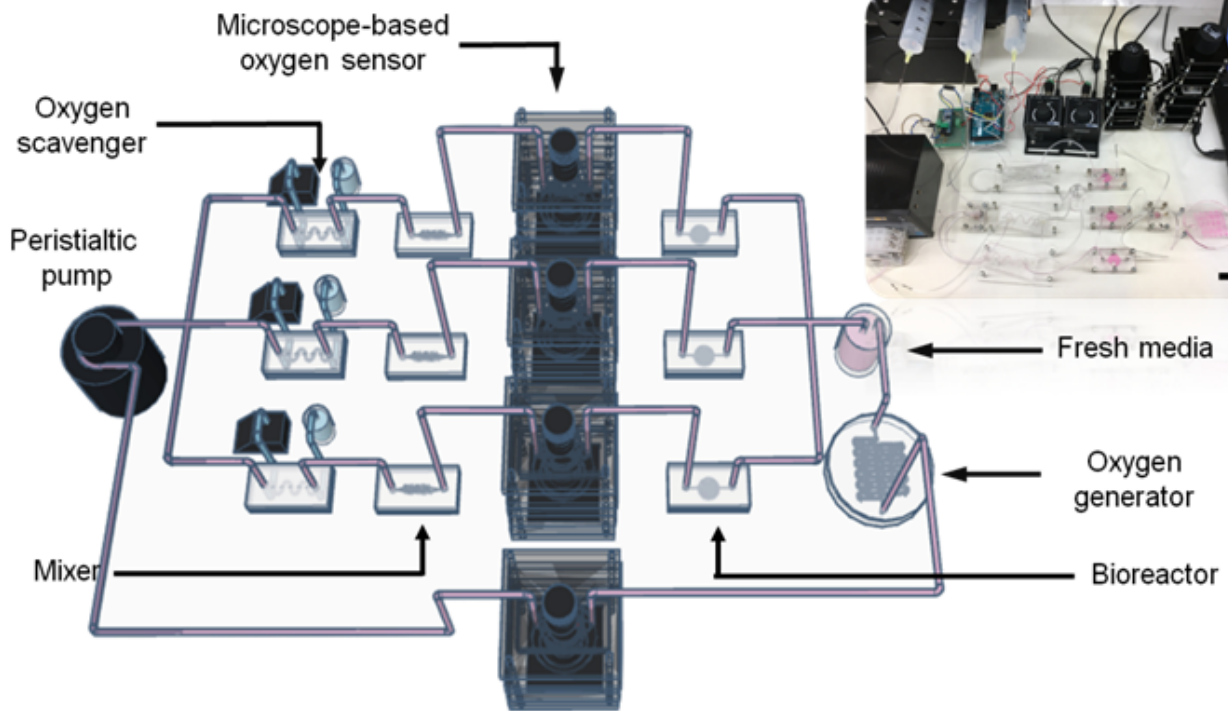


FIGURE 2.1. Schematic setups for closed-loop liver on chip platforms with different oxygen levels.

The system described in figure is constituted by three *scavenger chips* and three *bioreactor chips* working in parallel. In this way, culture media with different oxygen concentration can be provided to different kind of cells, according to their needs. The cell culture media is then mixed in a single container and passes through the *oxygen generator chip* in order to increase increase back the oxygen level and send it again to the *oxygen scavenger chips*.

It can be observed that the *Oxygen Scavenger chip* is characterized by two inlets and two outlets. This is because it is constituted by two adjacent channels, one reserved to the culture media flow, the other one to the scavenging solution flow. The scavenging solution need to have a variable flow rate. An Arduino code is implemented in order to control the scavenger solution flow rate through a peristaltic pump. Moreover, Arduino is used to control the two mini-microscope-based oxygen sensors, by commanding of taking interleaved images (samples) and sending them to the PC. A MATLAB code is implemented in order to analyse the samples from the mini-microscope

based optical sensor.

MINIMICROSCOPE BASED OXYGEN OPTICAL SENSOR

3.1 Introduction

Traditional oxygen quantification is based on the sample analysis by chemical, physical or instrumental methods. However, there is an increasing request for continuous monitoring, *in situ* and *in vivo* analyses, non-invasive measurements of O_2 concentration in biological systems. This has led to the development of new oxygen measurement methods.

Most of the first works on oxygen sensors were centred on Clark electrode, where the oxygen decrease is detected by measuring the electrical current. Electrochemical oxygen sensors own some disadvantages, for example they require a physical, conductive connection between the electrode and detector. This means that it can cause contamination of the solution to be analysed. Moreover they can cause the formation of oxygen-depleted regions.

Subsequently most of the focus has been in the incorporation of optical oxygen sensors, especially in microfluidics systems. Optical sensors have many benefits: easy miniaturization, may be used not in contact with solution, which means non-invasively or remotely, and do not consume oxygen. The optical sensor developed in this thesis project is based on the phosphorescence quenching. It is composed by a mini-microscope getting shot to a luminescence-based indicator (a dye sensible to oxygen) with culture media under analysis flowing above it, enlightened by a blue LED.

The luminescence indicator is embedded in a thin polymeric membrane. The luminescence of the dye is quenched by molecular oxygen present in the culture media. This is why the decrease of luminescence can be directly linked to the culture media concentration of oxygen.

The advantage in using this kind of sensor is that are not toxic, providing non invasive, real-time, in situ monitoring. Of course the package needs to be transparent in order to analyse the luminous intensity provided by the indicator.

One disadvantage is the temperature dependency of the quenching process. This is why the whole system needs to be placed inside an incubator set to 37°C , that is the best temperature for cells growing.

3.2 Phosphorescence quenching oxygen sensor

Optical techniques, especially phosphorescence based, are dominant. With these techniques, special "indicator substances" are the basis of the detection of oxygen levels.

Synthetic indicators, represented by oxygen sensitive dyes, are often used in order to test and detect the oxygen concentration of a specific sample. The indicator produces a response as an outcome of a photophysical process (the phosphorescence quenching) that is related to the oxygen level of the sample.

Large part of optical sensors for oxygen sensing is based on the concept of reversible luminescence quenching of the intensity of a luminescent indicator dye. The process consists in the transfer of energy from an excited state of an indicator molecule to a different molecule, for example oxygen, instead of being emitted as a luminescence photon.

Briefly, what is at the base of the measurement is the luminescence quenching caused by oxygen. When a collision occurs between the oxygen and the luminophore, the result is a non-radiative de excitation (dynamic quenching). The collision leads to an energy transfer from the luminophore excited state to the oxygen. This is followed by the energy transfer from oxygen ground state to its excited singlet state. The outcome is that the luminophore doesn't emit luminescence. The oxygen percentage is then measurable by measuring the luminescence signal decrease.

Luminescence: Luminescence is the light emission from an excited electronic state of a molecular species. There is a difference between the photoluminescence of an atomic species and a molecular species. In atomic species, the wavelength of excitation and emission are the same (resonance wavelength), while in molecular species, typically the emission is at a longer wavelength than the excitation.

The diagram that illustrates the radiative and non-radiative transitions related to photoluminescence in molecular species is an energy level diagram called Jablonski diagram. In order to understand the diagram is good to clarify that when the electrons are paired in an electronic state, this is the case of a singlet spin multiplicity. On the other hand, when the electrons are unpaired in an electronic state, is the case of triplet spin multiplicity.

Usually the ground state is indicated as S_0 and is a singlet state. Then there are the first and second excited states S_1 , S_2 , that are either singlet, and the excited triplet state T_1 .

According to the selection rule, the spin multiplicity should be preserved after excitation.

When absorption of light from a molecule occurs, an electron is promoted from the ground to an excited state by conserving the spin multiplicity. This means that triplet excited states are excluded in this step since the spin multiplicity is not conserved in this case.

After absorption, several non-radiative and radiative processes occur. As it can be observed in figure 3.1, during phosphorescence quenching the most important transition are the *Internal Conversion* and the *Intersystem Crossing*. Both of them are non-radiative transitions.

Internal conversion occurs when a molecule is excited to an excited singlet state characterized by a higher energy level than S_1 (for example S_2). In this case occurs a non-radiative relaxation to singlet state with lowest energy (S_1). This transition is among states where the spin multiplicity is maintained.

Intersystem crossing occurs when the relaxation is between states where the spin multiplicity is different. This kind of transition is less probable precisely because the spin multiplicity is not maintained. In the case under analysis, the presence of oxygen (that is a paramagnetic molecule) increases the probability of occurrence of intersystem crossing.

The non-radiative transitions described above occur in a very short time and release a very small amount of energy. All the remaining energy is dissipated in many way, radiatively (photons

emission) or not radiatively (thermal energy). The process that lead to quenching of luminescence is the non-radiative decay to the ground state, called non-radiative de excitation.

Photoluminescence consists in photons emission that occurs in such molecule while de-excitation. This is one potential physical effect arising from the interaction between matter and light.

The luminescent molecule gain energy in order to move from the ground state (S_0) to an higher energy level, that can be the electronic state 1 or 2 (S_1 or S_2), by absorbing a photon.

The transition takes place in approximately 10^{-15} seconds and the consequent de-excitation process can be observed in the Perrin-Jablonski diagram in figure 3.1.

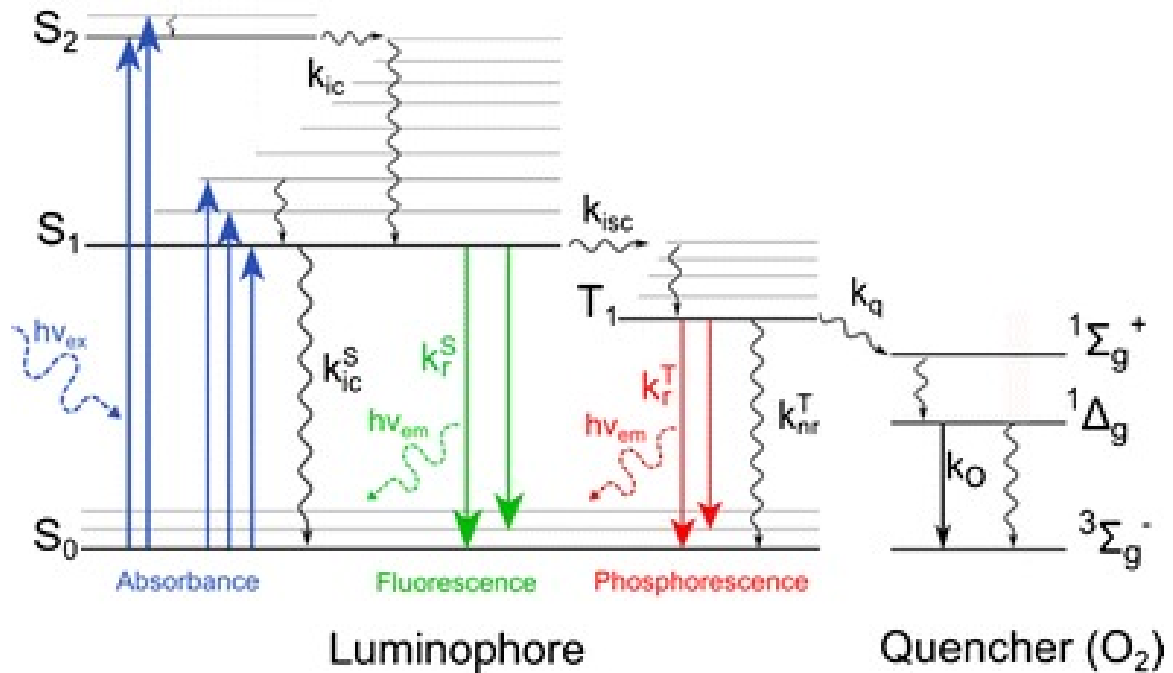


FIGURE 3.1. Jablonski diagram showing the phosphorescence quenching by O₂ process.

Briefly, after the photon absorption, the translation from the excited higher energy level to the lower level S_1 occurs. This process is a nonradiative transition and takes typically 10^{-12} seconds, generally is complete prior emission. From S_1 level, two possible de-excitation processes

are possible: *fluorescence emission*, spin-allowed transition without changes in multiplicity, that is highly probable; and *phosphorescence emission* from the lowest excited triplet state T_1 , this process needs non-radiative cross-system intersection between two iso-energetic vibrational levels that belong to electronic levels of different multiplicities (from S_1 to T_1), this is less probable. The strong atom presence within the indicator makes the probability of intersystem crossing increase, by promoting highly efficient phosphorescence.

When a molecule excited to an higher level goes back to the ground state, it performs emission of photons at a lower energy and higher wavelength with respect to the light that has been absorbed. Since phosphorescence emission takes place from a lower energy, the light emission is more accentuated for phosphorescence emission.

The quenching behaviour can be described by the Stern Volmer equation:

$$\frac{\tau_0}{\tau} = \frac{I_0}{I} = 1 + k_Q \tau_0 pO_2$$

where:

- pO_2 : partial pressure of oxygen
- k_Q : quenching rate constant
- τ_0 : excited-state lifetime at the pressure of interest
- I_0 : luminescence intensity at a known pressure

The Stern-Volmer equation can be expressed with regard to dissolved oxygen concentration rather than pO_2 , by using different units for k_Q .

Two different measurement methods can be used, since oxygen quenches both the excited-state lifetime and the luminescence intensity.

In this work, the method used involves the detection of the luminescence intensity.

3.3 Luminescence-based indicator and Detection of Luminescence intensity

The luminescence-based indicator used in this project is $[Ru(dpp)_3]^{2+}Cl_2$ -*tris(4,7-diphenyl-1,10-phenanthroline)ruthenium(II)* chloride, with a luminescence duration up to $6.4\mu s$ and a quantum yield of 0.3. This oxygen indicator is largely used, even though it presents some disadvantages.

The luminescence of this indicator is characterized by metal to ligand charge transfer (MLCT) process. Both emission and excitation bands of the MLCT sets are very large, which means higher allowance in the choice of the excitation source but difficulty in isolating the emission. In particular, the absorption of the Ru(II) chloride is placed in the blue part of the spectrum.

The phosphorescence of luminescent dyes is inclined to thermal quenching. Specially MLCT indicators show an high degree of thermal quenching. This means that the sensitivity to the oxygen depends not only on the nature of the compound but on the temperature. For this reason, all the measurements are taken within an incubator which keep the temperature steady at $37^\circ C$. The luminophore is turned on by a source of light excitation (blue LED). The source goes through a filter in order to choose the wavelengths that best match with the luminophore excitation spectrum. Moreover, an emission filter is used in order to remove any light external to the emission spectrum from the emitted luminescence intensity. After that, the luminescence intensity is detected by a camera, whose pictures are analysed by a MATLAB code.

3.4 Fabrication of optical oxygen sensor

In this work, the oxygen indicator is a fluorophore sensitive to oxygen, $[Ru(dpp)_3]^{2+}Cl_2$ -*tris(4,7-diphenyl-1,10-phenanthroline)ruthenium(II)* chloride (Sigma-Aldrich), that has the advantage of high photostability and moderate brightness. The maximum excitation is for a wavelength of $463nm$, and the emission is maximum for $618nm$. The luminophore powder is dissolved in ethanol, with a concentration of 1 mg/ml.

Since we need to use the dye for oxygen measures in aqueous solution, a thin layer of polydimethylsiloxane (PDMS) is deposited above the oxygen indicator. This layer is essential in

3.4. FABRICATION OF OPTICAL OXYGEN SENSOR

order to protect the dye to directly meet the solution and, at the same time, it allows the oxygen diffusion from the solution to the oxygen sensor. In order to excite the dye, an high power blue LED (M470L3, 470nm, 650mW, Thorlabs) is used.

Most of the system is fabricated in laboratory using the laser-cutter machine and poly(methyl methacrylate) (PMMA) sheets. The PMMA is a material that allows the oxygen isolation from the air. In this way it is possible to ensure that the oxygen concentration analysed is the one of the solution under analysis without interference of the air.

The optical oxygen sensor was fabricated using PMMA sheets. Briefly, two layers of PMMA sheets (3.25 mm in thickness) were cut using a CO₂ laser ablation system (VLS2.30, 30 W) operating at a wavelength of 10.64 μm at 30 W. The layers were combined using a thermal fusion method, in which both layers were clamped together and underwent thermal treatment in a vacuum oven at 130 ° C for 2 hours. The schematic and photograph of oxygen sensor are shown in Figure 3.2.

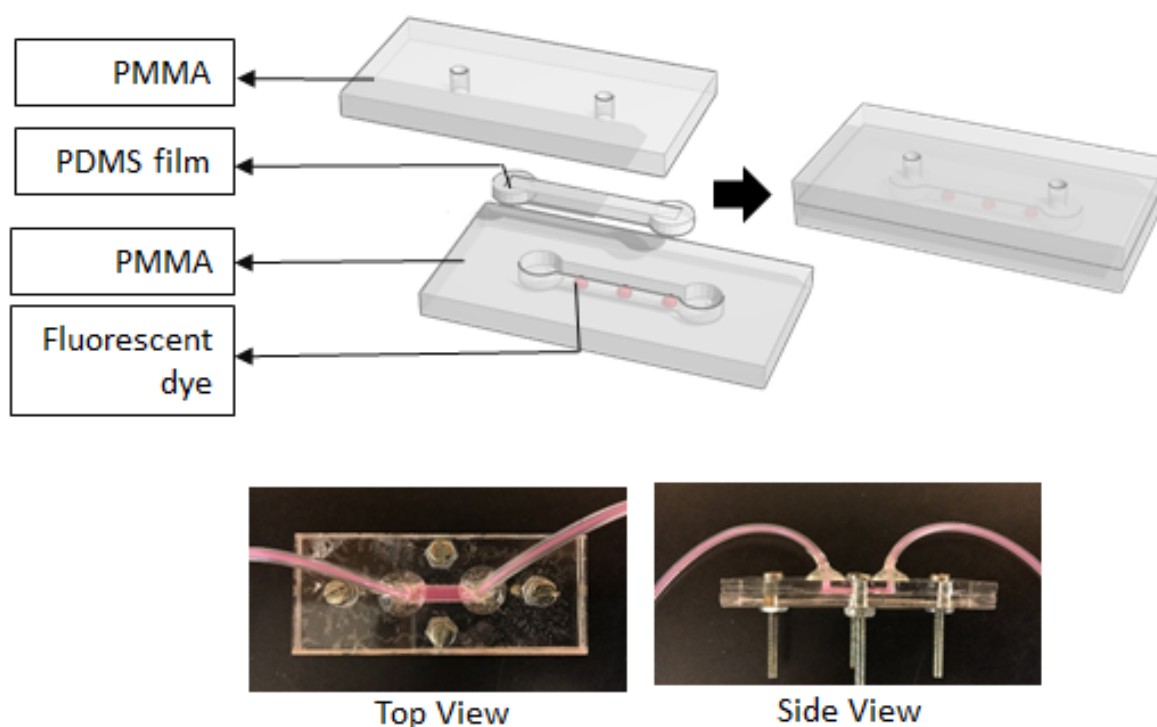


FIGURE 3.2. Schematic and photograph of a custom made oxygen sensor.

The mini microscope has a small form factor ($6 \times 6 \times 16 \text{ cm}^3$). It has been integrated with optical oxygen sensor. The minimicroscope was constructed using PMMA sheets ($\sim 3 \text{ mm}$ in thickness) including blue LED light, optical filters, PMMA based oxygen sensor, and a commercially available web camera disassembled with plastic casing. Nine rectangle PMMA frames were cut out using laser cutting system and mounted using screws/bolts. The top layer held the LED unit and optical filter for excitation light unit while the bottom layer held web camera and optical filter for emission light unit. The middle layer held the oxygen sensor which consisted of two PMMA layers sandwiched with oxygen quenchable fluorescent dye $[Ru(dpp)_3]^{2+}Cl_2 - tris(4,7\text{-diphenyl-}1,10\text{-phenanthroline)ruthenium(II)}$ chloride, $\lambda_{ex}/\lambda_{em} = 463\text{nm}/613\text{nm}$.

The schematic and photograph of the custom made minimicroscope-based oxygen sensor is shown in Figure 3.3.

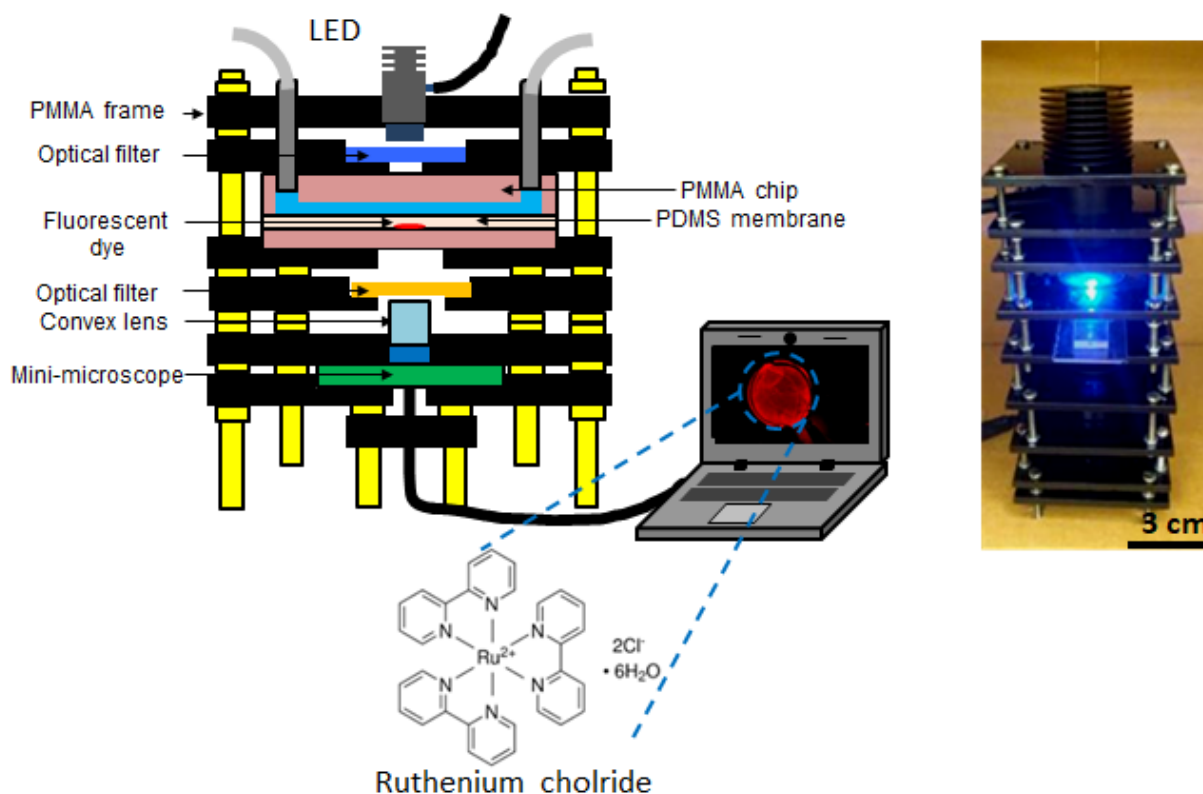


FIGURE 3.3. Schematic and photograph of the custom made minimicroscope-based oxygen sensor.

The microscope is able to capture the fluorescence images of the oxygen sensor using high energy blue LED ($\lambda_{ex} = 470nm$).

The minimicroscope has a maximal resolution of 1920 x 1080 pixels. The working distance was measured to be 35 mm by imaging the targets at preset distances from the oxygen sensor.

A custom-coded MATLAB software was carried out to capture and analyze the fluorescent images. Briefly, the captured images are imported into a MATLAB program, the fluorescence spots are cropped from the image, separated into separate R/G/B components and converted to fluorescence intensity values. It can be seen that the blue LED has a narrow wavelength of emission and provides a clear signal in R channel without interference in G and B channel (Fig. 3.4).

When the captured image is split into R/G/B component, the red emission component in the red channel (R) is easily retrieved with a relative intensity of 64, while intensity in green channel (G) and blue channel (B) are 0.24 and 0.08.

It can be concluded that a pseudo-colored image with minimal interference can be obtained, showing the mini-microscope can be applied for optical quantification of oxygen levels.

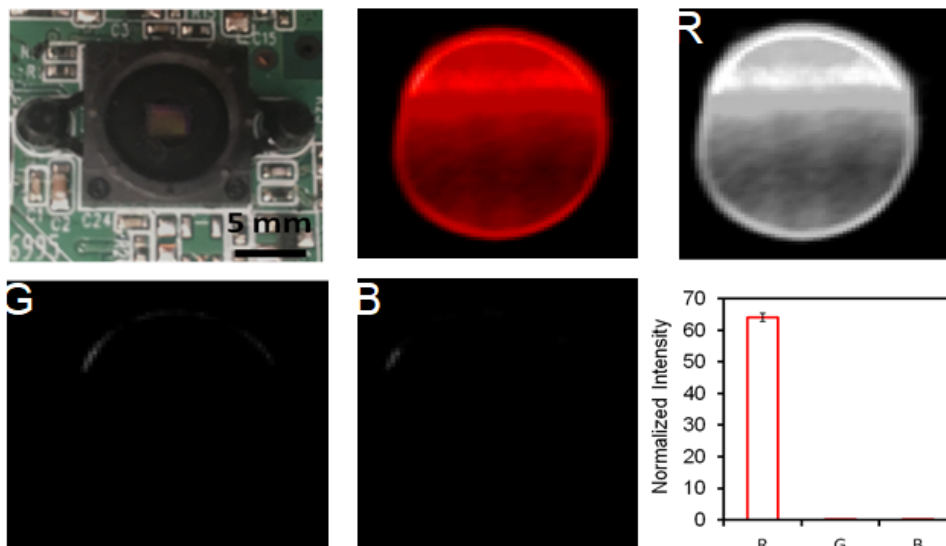


FIGURE 3.4. RGB configuration of the CMSO sensor for the minimicroscope and analysis of the separate R/G/B channels.

3.5 MATLAB code for luminescence intensity analysis

The MATLAB code is developed in order to evaluate the luminescence intensity of ruthenium dye beads inside the oxygen sensor.

The pictures obtained from minimicroscope are characterized by small dye areas (the beads) in a black background. As is explained in the previous section, the red emission component in the red channel has a much higher relative intensity than in green and blue channel. For this reason the picture obtained from the minimicroscope is split into R/G/B components and then only the R one is considered for the luminescence intensity analysis.

In order to have an higher accuracy, the beads areas are selected so that only the ones more reactive to light source are analysed and thus cropped from the whole image. The cropped areas are analysed and the average is computed in order to obtain the final luminescence intensity.

First, the base picture is read by using the *imread(filename)* function, inferring the format of the file from its content. This picture is stored as "base" since it will be the base from which the beads are detected and selected. An example of image obtained from the minimicroscope-based oxygen sensor is shown in Figure 3.5.

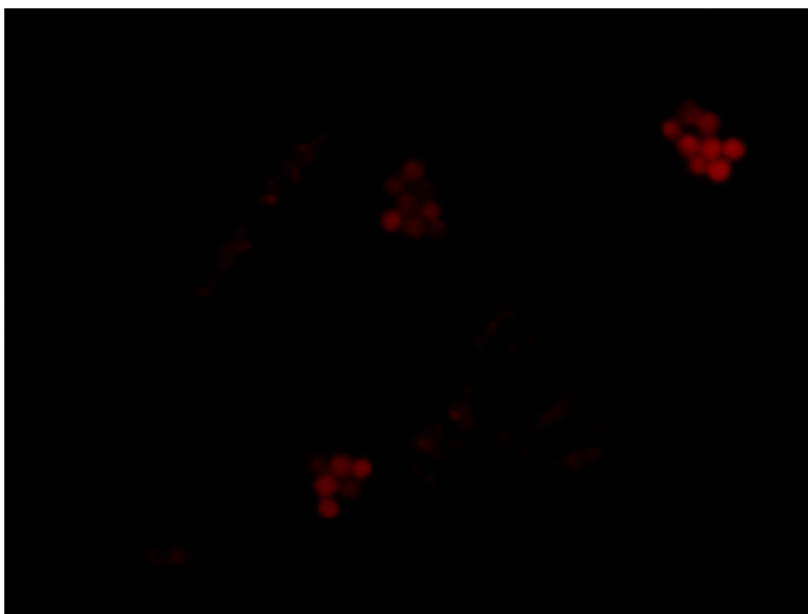


FIGURE 3.5. Example of ruthenium beads image from minimicroscope.

From the *base* image, only the red component is considered. MATLAB has three basic image types:

- Truecolor: arising out of digital cameras and broadly used in computer graphics
- Indexed and scaled indexed: frequently used to display scientific and engineering data with associated color scale representing the data units.

In this case we are dealing with Truecolor images. In a truecolor images, each image pixel is characterized by three values: the blue, red and green components. Truecolor images can be represented in MATLAB with a 3D array of size M - by - N - 3. Display functions in MATLAB and the Image Processing Toolbox treat such an array as a truecolor image.

Different shades of colors in RGB images are not obtained by using a palette. Each pixel color is given by combining blue, red and green intensities memorized in each color plane at the pixel's location.

RGB images are stored in graphics file format as 24 bit images, where blue, green and red components are 8 bit each.

The result is a potential of 16 million colors. The nickname "truecolor image" is precisely due to the precision with which an image can be replicated.

An RGB array can be of different classes: uint8, uint16 or double.

In an RGB array of class double, each color component value is between 0 and 1. A pixel displayed as black has color components equal to (0,0,0), and a pixel displayed as white has color components (1,1,1). The three color components for each pixel are memorized along the 3rd dimension of the data array. An RGB triplet is the three-element vector that specifies the intensities of blue, green and red components of the color. The first page of the 3D array contains the red components, the second page contains the green components, and the third page contains the blue components, as shown in Figure 3.6.

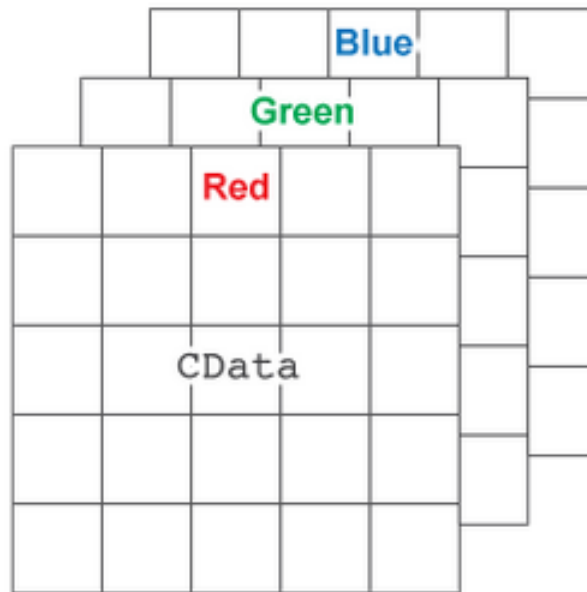


FIGURE 3.6. 3-D array of RGB triplets illustration.

In order to split RGB channels, it is sufficient to write:

```
img = imread('filename.png'); % Read image
red = img(:,:,1); % Red channel
green = img(:,:,2); % Green channel
blue = img(:,:,3); % Blue channel
```

Since only the red component needs to be considered, the *base* image is stored as *base = base(:,:,1)*. The resultant image is shown in Figure 3.7.

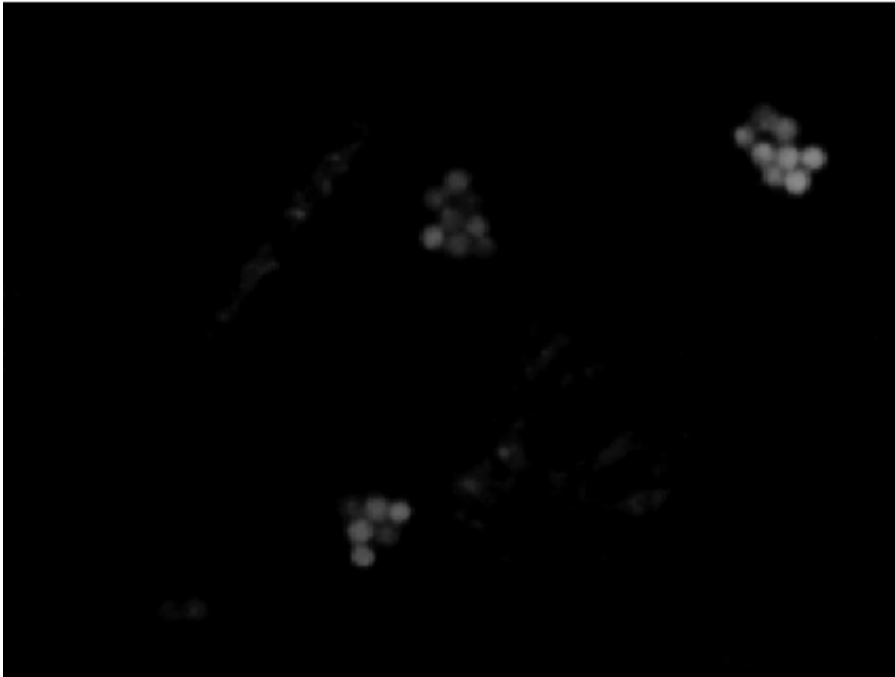


FIGURE 3.7. Example of base image.

By using the *graythresh(ImageName)* function, the global threshold is computed. The function uses Otsu's method, which chooses the threshold to minimize the intraclass variance of the white and black pixels.

Otsu's method, named after Nobuyuki Otsu, performs the clustering-based image thresholding. The algorithm assumes that the image includes two classes of pixels (background pixels and foreground pixels). In order to guarantee a minimal combined spread, the optimal threshold that separates the two classes is computed. This is useful to crop the beads areas.

The mask is obtained by using the function *im2bw(ImageName, threshold)*, where *threshold* is the value obtained from the *graythresh* function. The *im2bw* function turns the initial image in gray-scale to a binary image. This is performed by substituting all the input image pixels with a luminance higher than the *threshold* with the value 1 (white), while all the other pixels are replaced with the value 0 (black). An example of mask obtained is shown in Figure 3.8.



FIGURE 3.8. Example of mask image.

By using the function `regionprops(ImageName)` it is possible to measure the properties of image regions. In this case, the mask is analysed via this function, returning an array containing a struct for each object in the image.

The properties analysed are: area (of each white region), centroid (x and y coordinates of the centroid) and boundingbox (x and y bounds of the smallest rectangle enclosing the region).

From these properties, a vector of the areas and a vector of the centroid are created. The centroid array is sorted in x direction by using the function `sortrows(centroid,1)`. In this way it is possible to compute the average of x and y coordinates, obtaining the centre of the image. This is useful when cropping the borders is needed (if the oxygen sensor chip is not perfectly positioned it is possible that the image includes areas outside the chip). The base and mask obtained are then unique for one oxygen sensor chip. This first part of the code needs to be settled up for each oxygen sensor chip, but is needed as reference for the following images from the same sensor chip for which no more set up is needed.

At this point, the image under analysis is read by using the function `imread(ImageName)`.

The same steps performed for the *base* image are performed for the image under analysis. Only

the red component is considered, a second mask is created by using the same threshold level previously computed, the properties of the mask are evaluated and areas and centroid array are created. Again the average x and y coordinates are computed and the central part of the image is cropped.

How to select the beads to be analysed The cropped *base* mask is obtained and the properties of each region are evaluated. A new mask is created where, in correspondence of the centroid of each detected region, the value of the area is written in red. The value of the areas of the beads that the user wants to analyse are stored in an array called *goodareas*. In correspondence of these areas, the image will be cropped in order to be analysed.

An example of the mask just described is shown in Figure 3.9

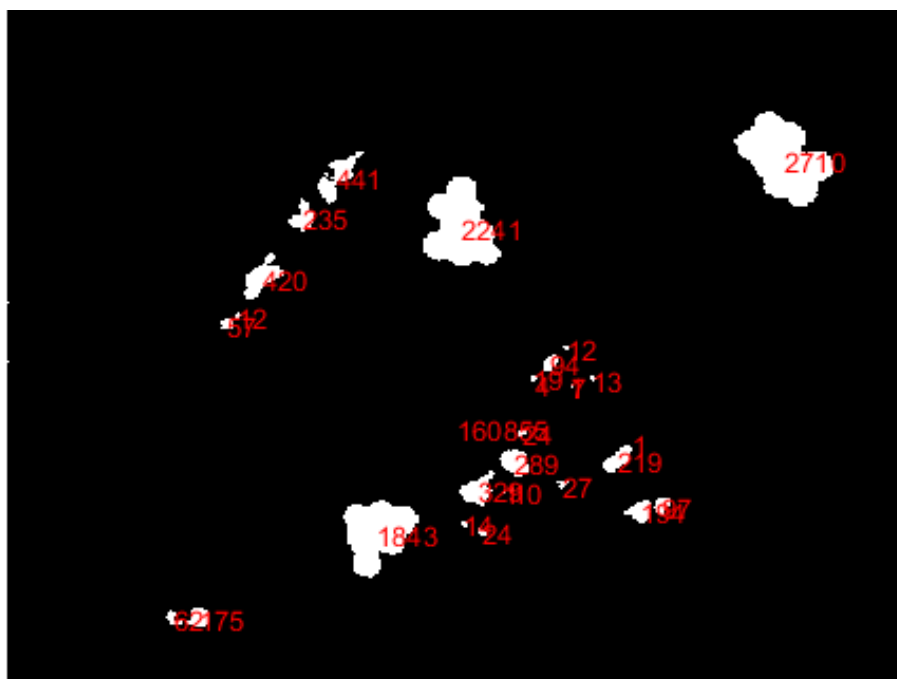


FIGURE 3.9. Example of mask image for dye beads selection.

For each selected bead area, centre coordinate are evaluated. The regions are cropped as shown in Figure 3.10.



FIGURE 3.10. Example of cropped bead areas image.

Finally the luminescence intensity value is computed by summing the value of every pixel inside the useful cropped areas. The value is then divided by the area of the cropped square.

Following the integral MATLAB code.

```
base=imread('image0.png'); %Gets BASE PICTURE
base=base(:,:,1); %Only considers red component
thresh=0.065*graythresh(base); %Sets the gray threshold
mask=im2bw(base,thresh); %Gets a mask using the threshold
regp=regionprops(mask); %Gets features (area, centroid, boundingbox)
areas=cat(1,regp.Area);%Gets area as vector
centroid=cat(1,regp.Centroid); %Gets centroid as vector
censort=sortrows(centroid,1); %Sorts centroid in x direction
con1=censort(1,1)
con2=censort(end,1);
basalcenty=round((con1+con2)/2); %Average of y-coordinate
con3=censort(1,2);
```

```

con4=censort(end,2);
basalcenx=round((con3+con4)/2); %Average of x-coordinate
crop1=uint8(zeros(575,814)); %NEEDS TO BE UINT8 so it can be added
for i=-(basalcenx-1):1:(575-basalcenx)
    for j=-(basalceny-1):1:(814-basalceny)
        %Crops the desired area
        crop1(basalcenx+i,basalceny+j)=base(basalcenx+i,basalceny+j);
    end
end
%%%%%%%%%%%%%%%%%%%%%%%%%%%%%%%%%%%%%%%%%%%%%%%%%%%%%%%%%%%%%%%%%%%%%%%%%
base2=imread('image1.png'); %Gets STUDY PICTURE
base2=base2(:, :, 1); %Only considers red component
mask2=im2bw(base2,thresh); %Gets a mask using the threshold
regp2=regionprops(mask2);
areas2=cat(1,regp2.Area);
centroid2=cat(1,regp2.Centroid);
censort2=sortrows(centroid2,1);
con21=censort2(1,1);
con22=censort2(end,1);
basalceny2=round((con21+con22)/2);
con23=censort2(1,2);
con24=censort2(end,2);
basalcenx2=round((con23+con24)/2);
crop2=uint8(zeros(575,814));
for i=-(basalcenx2-1):1:(575-basalcenx2)
    for j=-(basalceny2-1):1:(814-basalceny2)
        %Crops the desired area
        crop2(basalcenx2+i,basalceny2+j)=base2(basalcenx2+i,basalceny2+j);
    end
end

```

end

%%%

maskc=im2bw(crop1,thresh); *%Gets a mask using the threshold for CROPPED BASE*

regpc=regionprops(maskc);

areasc=cat(1,regpc.Area);

centroidc=cat(1,regpc.Centroid);

%%%SHOW Areas

hold on

for i=1:1:size(centroid)

text(centroid(i,1),centroid(i,2),**num2str**(areas(i,1)),'color','r')

end

%%%

goodareas=[2241;1843]; *%AREAS THAT CHANGE INTENSITY (best beads)*

goodcen1=[];

goodcen2=[];

for i=1:1:size(centroidc)

if (areasc(i,1)==goodareas(1,1))||(areasc(i,1)==goodareas(2,1))

 goodcen1=cat(1,goodcen1,centroidc(i,1)); *%Gets centroid-y for best areas*

 goodcen2=cat(1,goodcen2,centroidc(i,2)); *%Gets centroid-x for best areas*

end

end

%Final matrix with useful areas and centroid

finalareas=cat(2,goodareas,goodcen1,goodcen2);

sizegood=**size**(goodareas);

meanareas=**zeros**(sizegood(1,1),1); *%Vector of mean values*

for i=1:1:sizegood(1,1)

 subsumpic=0; *%Sum for each area mean value*

 centry=**round**(finalareas(i,2)); *%Coordinate-y of center of cropped region.*

```
centrx=round(finalareas(i,3)); %Coordinate-x of center of cropped region.
for j=-25:1:25
    for k=-25:1:25 %the number depends on how big are the beads
        %Adds the value for each pixel inside useful square
        subsumpic=subsumpic+double(crop2(centrx+j ,centry+k));
        crop2(centrx+j ,centry+k)=255;
    end
end
meanareas(i,1)=(subsumpic*2)./(51*51); %Mean value for each area
end
imshow(crop2)
meanpic=mean(meanareas) %Final average picture
```

3.6 Calibration Curve and Photobleaching correction curve

The luminescence intensity computed by the MATLAB code depends on the oxygen sensor itself: it depends on the number of dye beads , on their angle with respect to the LED and on their angle with respect to the camera. This means that for each fabricated oxygen sensor it is necessary to compute a different calibration curve.

The calibration curve computation is performed by preparing five different media solution, with different oxygen concentration.

The media solutions with different oxygen concentration are obtained by bubbling the sample of culture media with nitrogen for different period of time.

The dissolved oxygen concentration is, then, correlated to the electrochemical oxygen sensor (ISO-OXY-2) connected to a free radical analyser (TBR1025, World Precision Instrument). Once obtained five different samples with different oxygen concentration (0%, 5%, 10%, 15%, 20%), the luminescence intensity is measured by using the mini-microscope based oxygen sensor in order to obtain the calibration curve.

Since the result obtained with oxygen concentration of 15% and 20% were almost the same, the

graph in figure 3.11 consider up to the 15% oxygen level. In this way an almost linear curve is obtained. The equation obtained through the linear trend line is used in another MATLAB program, in order to convert the luminescence intensity measured in oxygen concentration percentage.

The calibration curve is computed for each different oxygen sensor in order to improve the accuracy of the measurements. An example of calibration curve is shown in Figure 3.11, where I_0 is the luminescence intensity obtained with a cell culture media with 0% of oxygen concentration, while I is the oxygen concentration measured.

The equation of the calibration curve linear trend obtained is used later for the evaluation of cell culture media oxygen concentration during the next experiments.

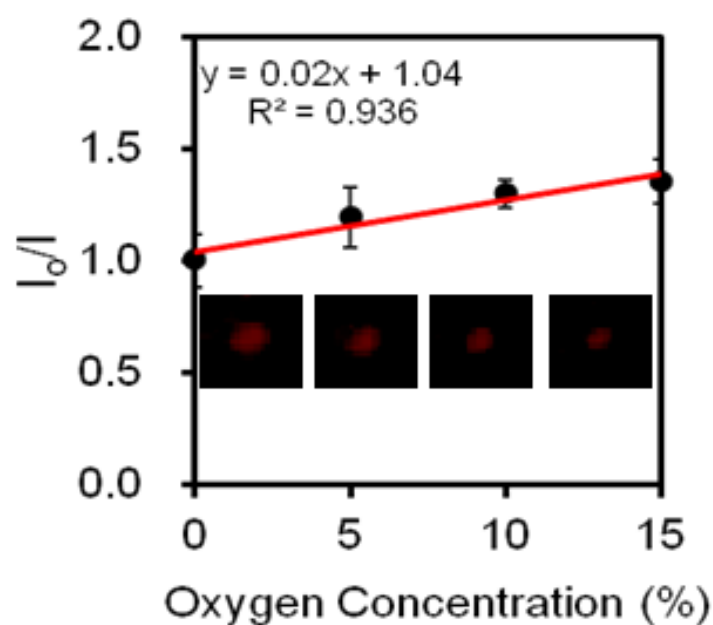


FIGURE 3.11. Oxygen sensor calibration curve.

Another important aspect that must be considered is the *photobleaching*.

Photobleaching is the photo-induced degradation of the fluorescent capacity. Molecules in excited states (S_1, S_2 or T_1) definitively lose their fluorescent capability due to photobleaching, this leads to an irremediable reduction of the number of fluorochromes that can be excited from the ground state S_0 .

3.6. CALIBRATION CURVE AND PHOTBLEACHING CORRECTION CURVE

Photobleaching is an undesired effect, since it suppresses possibly useful information.

There are several ways to minimize photobleaching, for example by minimizing the time of light exposure or the intensity of light source, which on the other side leads to a reduction of the fluorescence signal.

The ideal is to get the photobleaching curve for the correction of results obtained in different conditions.

Photobleaching curve can be modeled as a curve characterized by a negative exponential trend. The curve can be expressed as:

$$I(t) = Ae^{at}$$

where $I(t)$ is the intensity and is directly related to the fluorescence level.

In order to obtain this curve, using a cell culture media with 0% oxygen concentration, measurements are taken every 30 minutes for four hours. From this experiment, the photobleaching correction curve is obtained and is shown in figure 3.12.

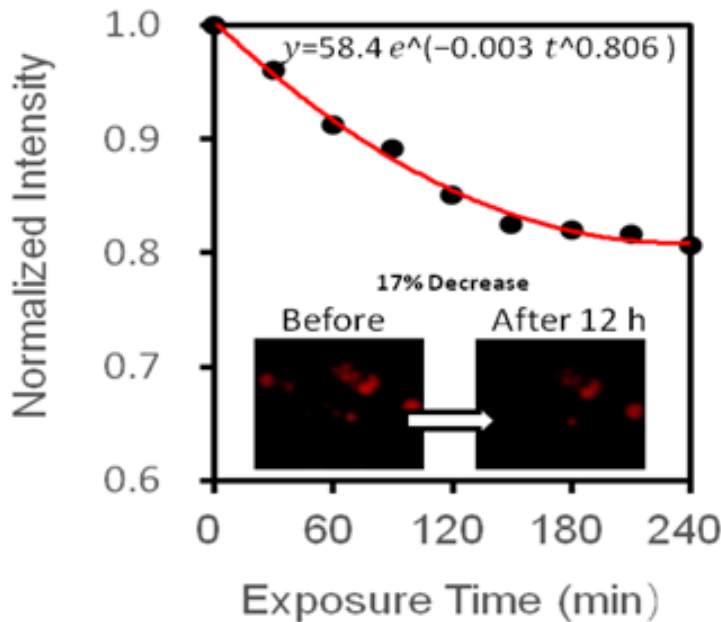


FIGURE 3.12. Photobleaching correction curve.

OXYGEN SCAVENGER CHIP

4.1 Introduction

The *Scavenger chip* is the chip dedicated to the reduction of the oxygen concentration in cell culture media, in order to provide to cells the proper oxygen level that depends on the cell type and can vary from 3% to 13%. The chip needs to be able to reduce the oxygen level of culture media in an adjustable way, in order to obtain different oxygen levels.

In latest years, many methods have been evolved to monitor gaseous surroundings to analyse cell behaviours under several oxygen levels.

In order to study cellular behaviour in low oxygen levels, the most prevalent tools are hypoxia chamber and hypoxia workstation.

Hypoxia chamber is a decompression chamber used to simulate low oxygen concentration conditions. It allows to obtain an hermetic gas and seal mix in a specified percentage to set the appropriate oxygen level. It is possible to put it in an incubator and there is no need of other specialised equipment, but it can guarantee just a single gaseous level at once and the oxygen is never equally distributed. Moreover, hypoxia chamber needs to be opened in order to change culture media at each time; this allows oxygen changes with external air by breaking gaseous equilibrium.

Hypoxia workstation is a kind of incubator where the oxygen level is constantly monitored and adjusted by a real-time feedback system. Hypoxia workstation is inclined to give an accurate and uniform oxygen surrounding. But it is also characterised by a large volume and by an expensive cost, these are obstacles for its application in laboratory.

The methods described usually need complex instrumentation beside a large amount of gas delivering. On the other hand, is very easy and efficient to directly add an oxygen scavenging agent in cell culture media in order to control oxygen tension. The disadvantage of this method is that adding a chemical compound will alter the medium compositions and influence cellular responses.

Relevant attempts have been made by developing various microfluidic devices in order to allow adjustable gaseous condition.

Microfluidic techniques overcome the limits of the previously described traditional methods and provides the opportunity to observe gaseous in real time and at microscale level. Former research have mentioned that nitrogen-oxygen mixture or pure nitrogen was directly pumped into microchannels to quickly reach the balancing of gas exchange in the contiguous channels, thanks to a barrier of PDMS, a material with high oxygen diffusion that will be described in detail later. However, with this method it is possible to have unwanted bubbles and that medium dry out inside the chamber, by reducing the repeatability.

In order to modulate oxygen, on-chip reactions consuming oxygen can be used.

This method has the advantage of eliminate the necessity for pressurised gas containers.

The most used method for oxygen monitor in microfluidics devices is the diffusion from a control channel through a thin PDMS membrane, that is gas-permeable, into the channel dedicated to cell culture media. The liquid in the control channel presents a different concentration of oxygen with respect to the media channel, leading to a diffusion of the oxygen from the media channel to the adjacent control channel. In this way it is possible to monitor the dissolved gas surrounding sustained by the cells.

The disparity between the oxygen level of the control channel and the oxygen level of the culture media channel combined with the high permeability of PDMS, lead to the creation of a gradient in the cell chamber. The flow rate of the control channel fluid is generally maintained by syringe

pumps. The media flow rate in the adjacent channel is maintained at a lower value than the control channel fluid in order to allow the creation of a steady oxygen gradient in the cell chamber. Skolimowski and his co-workers introduced the oxygen scavenging agents in order to lead to oxygen gradients by injecting $0.1\text{mM } \text{CoSO}_4$ with 10 % sodium sulfite solution.

Wang et al. demonstrated the generation of an oxygen gradient inside a channel. An oxygen scavenging agent that flows in a channel generates an oxygen gradient. Oxygen is mostly depleted in the middle of the channel and near to the gas impermeable wall and is reconstituted from the surrounding PDMS bulk.

4.2 Scavenger chip design

In view of the previous scientific research, the scavenger chip designed for this project is based on two channels engraved in two PMMA layers, divided by a thin membrane of PDMS.

The bottom channel is reserved to the oxygen scavenging liquid consisting in a Na_2SO_3 solution (10% sodium sulfite with 0.1 mM CoSO_4 as a catalyst) which consumes oxygen from the culture above. The top channel is reserved to the culture media. The flow rate of the culture media is fixed, while the flow rate of the sodium sulfite solution can vary across a range.

By increasing the sodium sulfite solution flow rate, the oxygen concentration reduction of the culture media increases as well. The expectation is that from a culture media with 21% of oxygen at the inlet of the scavenger chip, it is possible to obtain a culture media with a percentage of oxygen that can vary from the 13% to the 3% at the outlet.

In order to overcome the problem of the creation of an oxygen gradient within the channel, a *mixer* chip is designed to obtain culture media with homogeneous oxygen concentrations.

Mixing solutions in microchannels is very tough. In these channels the flows are generally laminar in typical operating conditions; there is no spontaneous oscillations of speed that mix fluids in turbulent flow, moreover the molecular diffusion across microchannel is very slow.

Physically flows in microfluidic channels have low levels of the Reynolds number ($Re = Ul/v < 100$, where U is the flow speed average, l is the cross-sectional dimensions, v is the kinematic viscosity

of the liquid). At low Re , in smooth channels, pressure flows are uniaxial and laminar, this means that the material is mixed between flows in a diffusive way.

In uniaxial flows, the distance along the length of the channel needed in order to mix can be very long.

Cross-sectional components are needed in order to reduce the mixing length.

The creation of cross-sectional flows in micro-channels allows the development of chaotic flows useful in microfluidic structures.

In Figure 4.6 is shown the mixer design, based on schemes of grooves on the bottom of the channel.

In order to produce a chaotic flow, the fluid is subject to a recurrent series of rotational flows. By changing the configuration of the grooves as a function of axial position in the channel, the sequence of local flows is obtained: the variation in the direction of the herringbones between half cycles exchanges the positions of the rotation centers and the up and down-wellings in the transverse flow.

Two regions of ridges compose one mixing cycle; the herringbones asymmetry direction changes with respect to the midline of the channel from one area to the next.

4.3 Materials

The two channels are engraved in two PMMA layers.

Poly(methylmethacrylate) (PMMA), also known as acrylic or acrylic glass, is a colourless thermoplastic. It is typically used in form of sheets as a shatter-resistant alternative to glass. Due to its tensile strength, transparency, flexural strength and tolerance to UV, PMMA can be an economical alternative to polycarbonate (PC).

For this work, PMMA is a very attractive material due to its low oxygen permeability, that prevents oxygen diffusion from the atmosphere in order to ensure the oxygen diffusion to be confined across the two channels. Moreover, PMMA is a polymer with high optical transparence and biocompatibility, that is an advantage for the use in optical sensor chip fabrication. The PMMA is, in fact, characterized by an oxygen diffusivity of $0.25 \cdot 10^{-11} m^2/s$.

The membrane between the two channels is made in **Polydimethylsiloxane** (PDMS).

The property of PDMS (a silicon elastomer) makes it very desirable for microfluidics components development in biomedical applications. It is thermally stable, chemically inert, permeable to gases, simple to handle and manipulate, lower cost than silicon.

PDMS is largely used in fabrication of microfluidic chips in several biomedical researches due to its excellent biocompatibility and well characterized oxygen diffusivity, characterized by an oxygen diffusivity of $400 \cdot 10^{-11} m^2/s$.

Oxygen-permeable PDMS membranes inside oxygen-impermeable (PMMA) microdevices is used for the transfer of oxygen from cell culture media to establish oxygen gradients within cell culture chambers.

4.4 Fabrication of Oxygen Scavenger chip

A CO_2 laser ablation system (VLS2.30, 30 W) operating at a wavelength of $10.64 \mu m$ at 30 W, with an X-Y platform regulated in Z-axis, was employed to create microchannels in transparent PMMA.

Laser ablation system is the process of removing material from a surface by irradiating it with a laser beam.

The software used to interface the CO_2 laser cutter machine is VLS.2.30.

Interface is needed in order to regulate the power, resolution and speed of the laser scanner. The design of the geometries to be cut have been realized by using CorelDRAW Graphics Suite X5 software. Then the designs have been sent to VLS.2.30, that converts the received design in series of control signals that command the servo motors of the laser ablation device and the attached laser head from micromachining of PMMA layers.

The geometry of produced microchannels in PMMA depends on thermal diffusion. Generally, the depth of the microchannel is established by the intensity and speed of heat dissipation in the matter. Due to the low thermal diffusivity of PMMA, the microchannel cross section is mainly determined by the laser intensity distribution.

In order to maximize the engraving efficiency, the radiant fluence (optical energy delivered per

unit area), beam speed and Z-axis of the X-Y platform of the CO_2 laser equipment have been optimized.

The fluence values varied from 96mJmm^{-2} to 390mJmm^{-2} at a constant beam speed (0.8mms^{-1}) and Z-axis (8.0 mm); the laser ablated depth of the PMMA matrix linearly increases from $278\mu\text{m}$ to $1234\mu\text{m}$. Laser ablated depth exponentially decreases from $1994\mu\text{m}$ to $587\mu\text{m}$ as the beam speed increases from 0.3mms^{-1} to 1.3mms^{-1} at a constant beam fluence (240mJmm^{-2} and Z-axis (8.0 mm) (Figure 4.1).

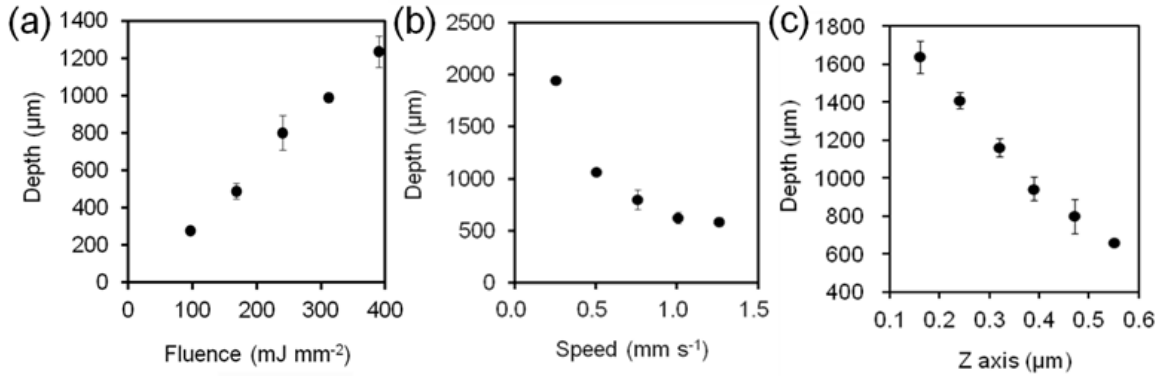


FIGURE 4.1. Optimization of CO_2 laser radiation fluence and beam speed for ablating plastic matrix (nominal thickness=3.0 mm). (a) Depth of the ablated regions as the laser beam fluence varied at a constant beam speed (0.76 mm s^{-1}) and Z-axis (8.0 mm); (b) Depth of the ablated region as the laser speed was varied at a constant fluence (249 mJ mm^{-2}) and Z-axis (8.0 mm); (c) Depth of the ablated regions as the Z-axis varied at a constant fluence (249 mJ mm^{-2}) and beam speed (0.76 mm s^{-1}) ($n=3$).

The laser beam is characterized by a Gaussian intensity distribution.

For a focused CO_2 laser beam, the typical cross section generated in PMMA is a Gaussian-like section.

Comparing two laser beam with the same power, the one unfocused has a lower peak energy intensity, a lower engraving depth and a wider spot size in the ablation with respect to a focused laser beam. Therefore, the engraved channels have been adjusted by varying Z-axis to create focused and unfocused laser beams by creating curved fluidics channels of different shapes in PMMA.

The curve of the channel is related to the unfocused height: the curvature of the channel enlarges as unfocused height increases.

In order to cut the PMMA sheet and produce layers of the needed size, a focused laser beam has been used. In order to engrave a channel in the PMMA layer obtained an unfocused laser beam has been used.

As it is shown in Figure 4.1(c), the laser ablated depth decreased from $1641\mu\text{m}$ to $565\mu\text{m}$ as a constant of beam fluence (240mJmm^{-2}) and speed (0.8mms^{-1}).

Figure 4.2 illustrates the photographs of the PMMA cross-section after laser ablation. The optimized ablation engraving of fluence, beam speed, and Z-axis are optimized at 240mJmm^{-2} , 0.8mms^{-1} and 8.0mm .

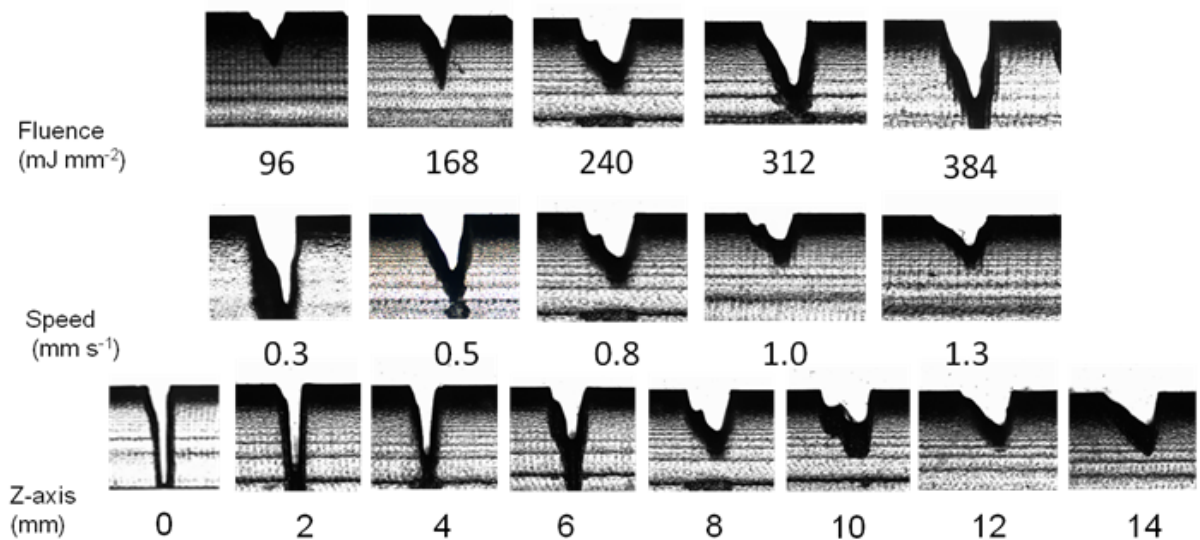


FIGURE 4.2. Photographs of laser ablated cross-sections of plastic matrix.

The CO_2 laser beam makes the temperature increase of the PMMA irradiated spot. The PMMA spot melts and then vaporizes, this generate the creation of microcavities in the surface. All the engraved microfluidic channels are treated with chloroform to remove microcavities with improved surface smoothness.

Smooth engraved channels have been obtained using chloroform vapour followed by thermal treatment. The engraved channels have been exposed to chloroform vapor at room temperature

for 4 minutes, after that they have been thermal treated at 70°C for 30 min.

This is a critical step for PMMA channels exposed to chloroform vapor. Compared with microchannels before and after treatment, the smoothness of the surface has been improved, after the debris has been removed (Figure 4.3).

The smooth surface would eliminate roughness and ensure hydraulic tightness and fluid seal.

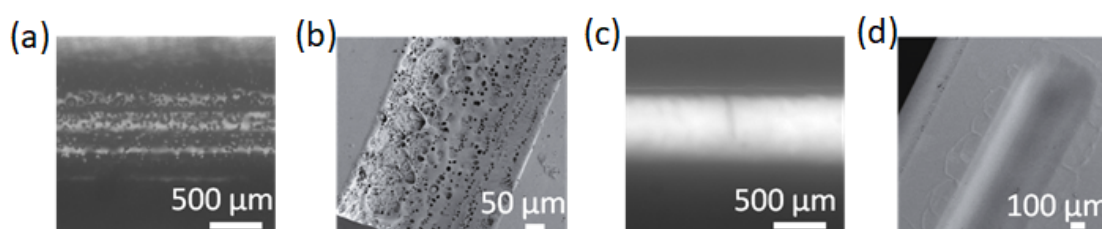


FIGURE 4.3. Optical and SEM images of laser engraved microchannels (a) and (b) before and (c) and (d) after chloroform treatment.

In order to separate two microchannels of PMMA chip, a PDMS membrane has been applied in between.

The silicone elastomer has been spin-coated on to a clean plastic substrate at different rate, by obtaining different thickness.

By decreasing the thickness of the PDMS membrane increases the oxygen diffusion across the two channels. The rates tested are 500 rpm for 30s, followed by 2000, 3000, 4000, 5000 rpm for 1 min.

The thickness decreases by increasing the rate as shown in Figure 4.4.

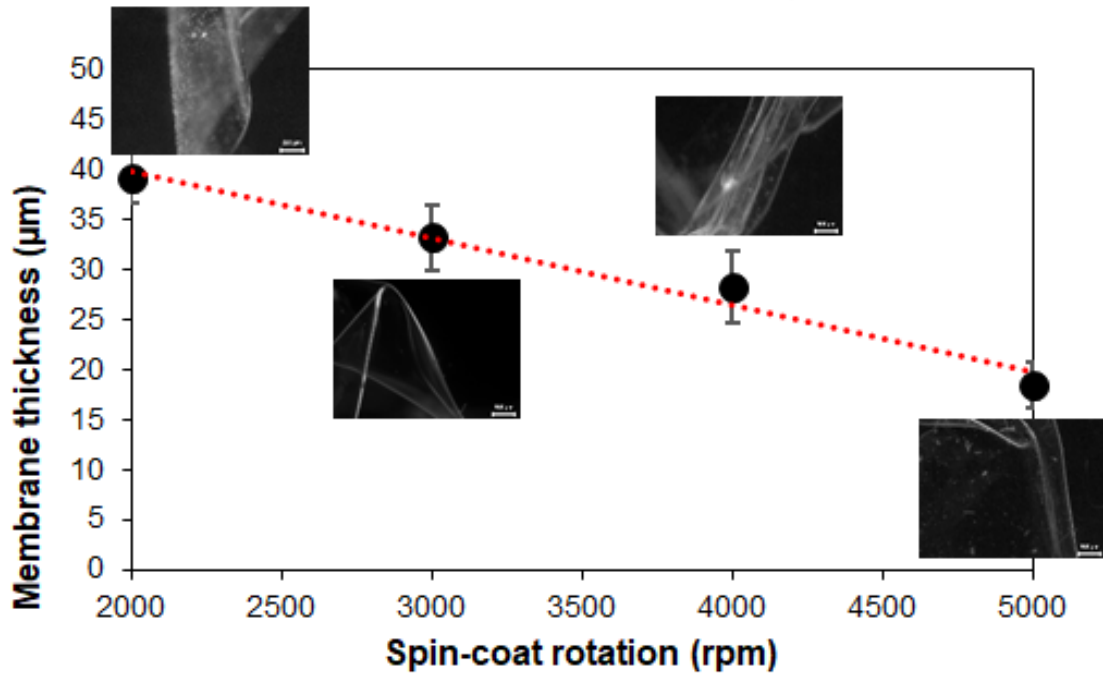


FIGURE 4.4. PDMS membrane thickness graph with respect to spin-coating rate, with related SEM images.

The final spin-coating rate is chosen equal to 5000 rpm, obtaining a PDMS thickness of $18.46\mu m$.

This membrane thickness allows to achieve the lower final concentration of oxygen at the outlet of the scavenger chip, without risking the break of the membrane.

Then the substrate coated with the silicone elastomer has been baked for 2 hours at $80^{\circ}C$. Subsequently, the PDMS membrane has been transferred from the substrate to the engraved PMMA chip, adequately positioned to cover the microchannel and sandwiched between two pieces of PMMA layers.

The layers have been attached together using a thermal-fusion bonding method, in which both layers have been clamped together and kept in the vacuum oven at $130^{\circ}C$ for 2 h.

The developed scavenger chip can be observed in Figure 4.5.

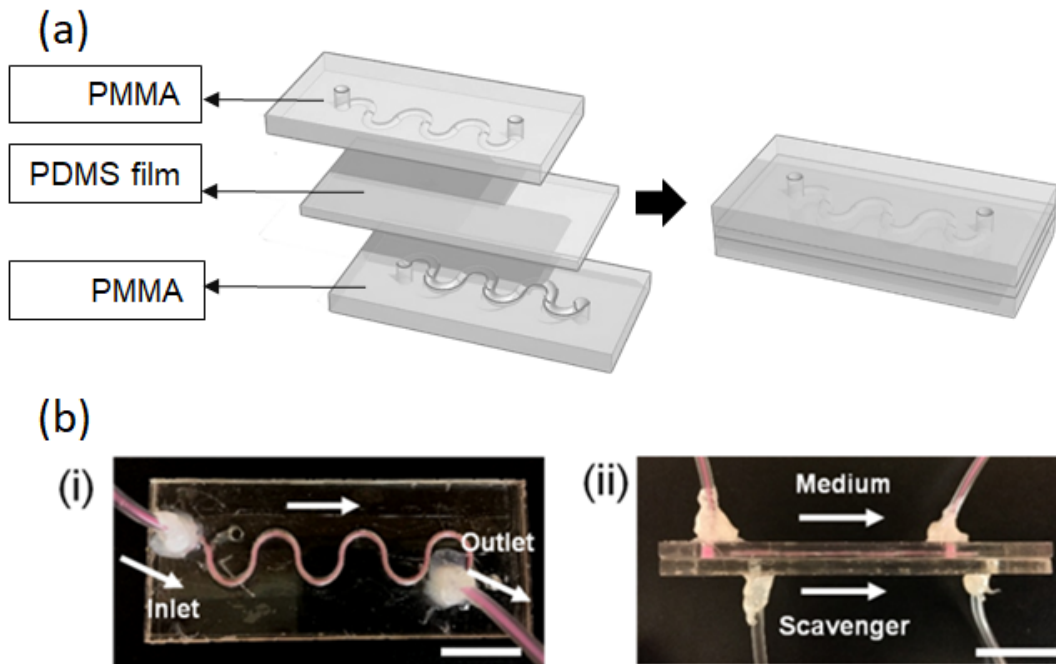


FIGURE 4.5. Modules for oxygen scavenging control. (a) Structure of oxygen scavenger which is consisted of three layers: two microfluidic PMMA layers and a sandwiched PDMS membrane. (b) Photographs of oxygen scavenger: top view and side view. Scale bar=1.5 cm.

To generate the culture media with homogeneous oxygen concentrations, a chaotic mixer has been designed.

The mixer chip is based on patterns of grooves on the bottom part of the channel, as can be seen in Figure 4.6.

Two layers of PMMA sheets (3.25 mm in thickness) have been cut using a CO₂ laser ablation system (VLS2.30, 30 W).

The layers have been attached together using a thermal-fusion bonding method, in which both layers have been clamped together and underwent thermal treatment in a vacuum oven at 130°C for 2 hours.

For the final assembly of the mixer, PVC tubes (3 mm for outer diameter) have been fixed to the mixer using epoxy adhesive.

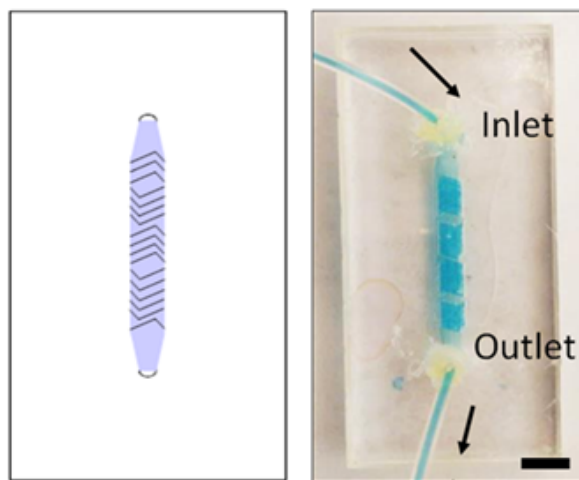


FIGURE 4.6. Chaotic mixer. Scale bar = 1 cm

4.5 Scavenger test

The scavenger solution has been prepared by bubbling PBS (phosphate-buffered saline, a buffer solution commonly used in biological research since buffer helps to maintain a constant pH) with pure nitrogen for at least 30 min in order to remove the dissolved oxygen from the solution.

After that, the sodium sulfite powder has been dissolved in PBS with a concentration varying from 0.02 to 0.2 g/mL.

$CoSO_4$ in concentration of 4 wt% has been used as the catalyst.

In the bottom side of the scavenger chip, Na_2SO_3 solution has been injected, while in the top side pure medium flowed with an initial oxygen concentration of 21%.

The oxygen scavenger chip has been connected to two syringe pumps.

The inlet of the top channel has been connected to a syringe pump with a flow rate of $200\mu Lh^{-1}$ and the outlet of the channel has been connected to the chaotic mixer.

The bottom channel has been used to infuse Na_2SO_3 solution with flow rates varying from 1000 to $2000\mu Lh^{-1}$.

In Figure 4.7 the scheme of the oxygen scavenger connected to the minimicroscope.

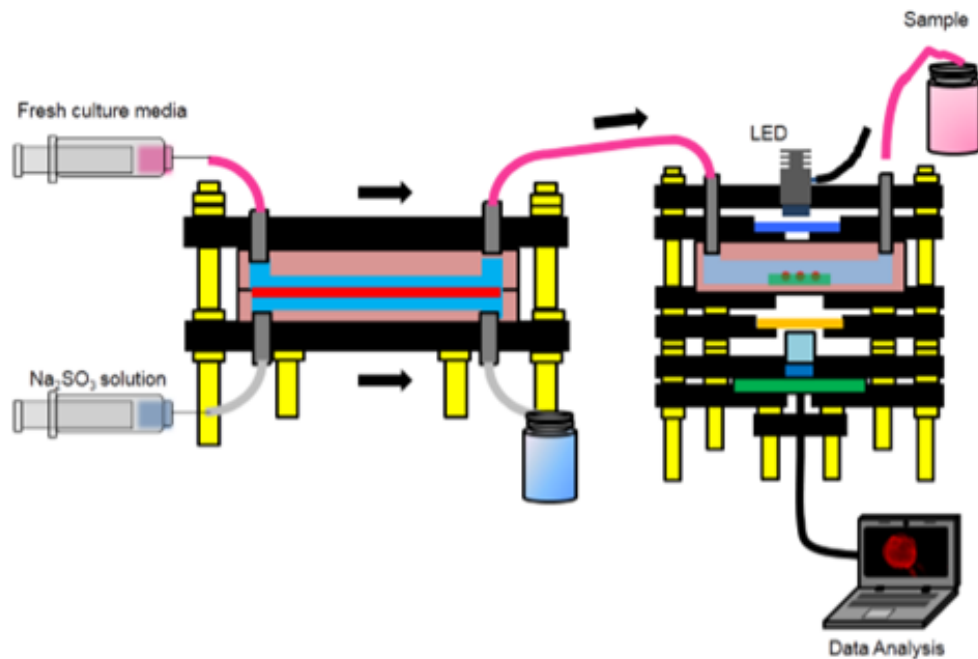


FIGURE 4.7. Scheme of the oxygen scavenger connected to the minimicroscope.

The scavenger chip has been tested for different scavenger solution flow rates and for different concentration.

The culture media passes through the top channel of the chip, with an initial concentration of 21% of oxygen.

At the outlet, the scavenger chip is connected to the chaotic mixer in order to obtain an homogeneous oxygen concentration.

Once mixed by the chaotic mixer, the media passes through the optical oxygen sensor previously described.

The media is then analysed by the MATLAB code, in order to verify a reduction of the oxygen concentration at the outlet of the scavenger chip.

Figure 4.8 shows the effects of the different concentrations of sodium sulfite solution and the flow rate on the oxygen level after cell culture media flows through the scavenger chip.

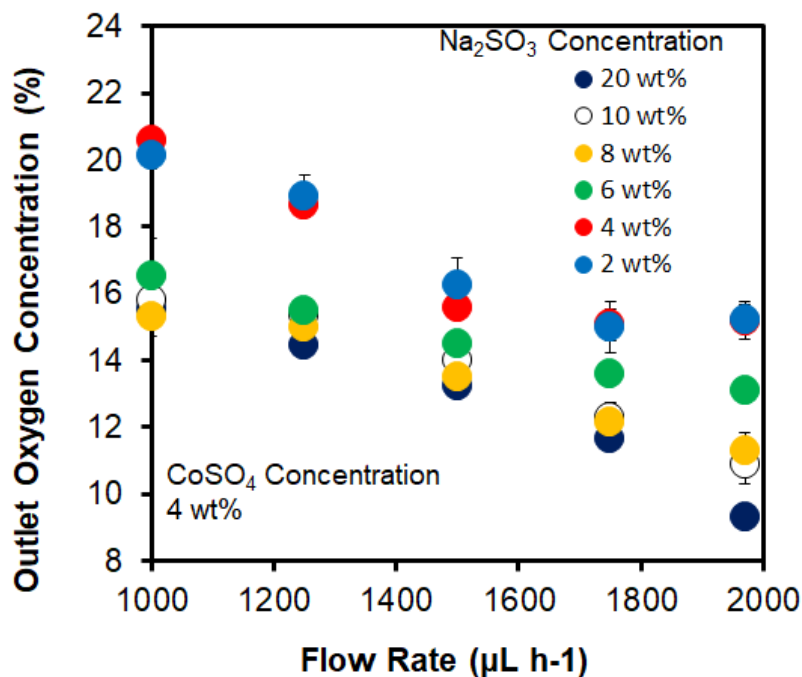


FIGURE 4.8. Outlet oxygen concentration as a function of flow rate within the bottom microfluidics with the Na_2SO_3 concentrations varying from 2 wt%-20 wt%.

It is observed that the $2000\mu\text{Lh}^{-1}$ flow rate results in the lowest oxygen concentration, being $9.3 \pm 0.6\%$ for the 20 wt% solution. While with a flow rate of $1000\mu\text{Lh}^{-1}$ the oxygen concentration is $15.6 \pm 0.5\%$ for the same concentration of Na_2SO_3 .

For the lowest sodium sulfite concentration (2 wt%), it can be observed that at a flow rate of $1000\mu\text{Lh}^{-1}$, oxygen level decreases only to $20.1 \pm 0.4\%$ achieving $15.2 \pm 0.4\%$ at the maximum flow rate ($2000\mu\text{Lh}^{-1}$).

These results indicates that 8, 10 and 20 wt% are the most suitable Na_2SO_3 concentrations for further experiments involving the cells culture in bioreactor.

The results are good for this project since we need an oxygen concentration at least lower than 13%.

Once the ability of the scavenger chip in decreasing the oxygen concentration in culture media has been tested, the next step consisted in test the stability of the scavenged oxygen.

The aim is to ensure that the oxygen concentration is maintained stable at the lower level with time.

The stability of scavenged oxygen with time has been evaluated by using the 10 wt% Na_2SO_3 solution and flow rate of $2000\mu Lh^{-1}$.

Results in Figure 4.9 show that the oxygen concentration is stable after 3 hours, remaining between 9 and 11 %.

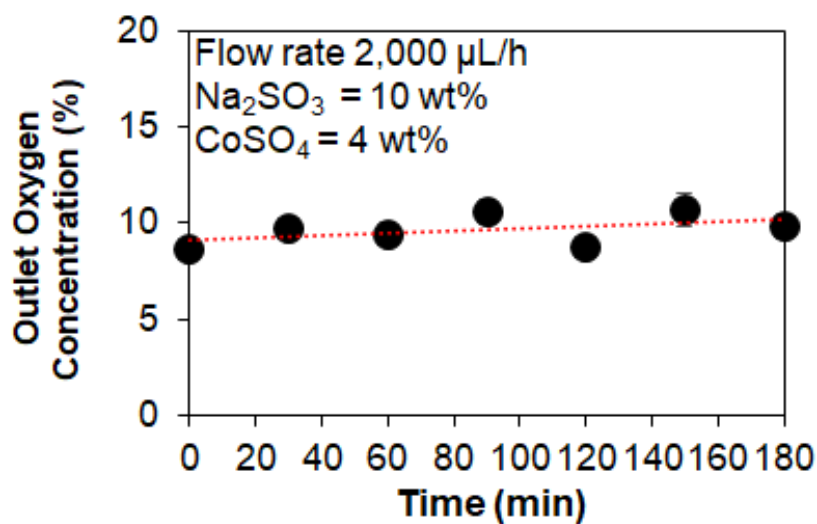


FIGURE 4.9. Stability of the oxygen scavenger with a prolonged time of 180 min.

Results presented here have shown that the scavenger chip, with Na_2SO_3 solution, is suitable to decrease the oxygen level.

LIVER-ON-CHIP BIOREACTOR

5.1 Introduction

Bioreactors are instruments used in the field of tissue engineering to grow and lead the development of tissue engineered constructs. More specifically, bioreactors are systems dedicated to *in vitro* culture, designed in order to modify some basic physiological events, such as cell structure, mechanical properties, function and survival along the tissue. The cell survival is assured in bioreactors thanks to proper supply fundamental nutrients by using tissue engineered construct in 3D.

By applying mechanical or chemical stimuli it is possible to lead tissue organization, structure and functions.

In Biomaterials and tissue engineering fields many progresses have been performed, leading to significant development with the aim of tissue constructs generation from human cells, in order to mimic cell interactions.

In particular, microbioreactors are fabricated by using microfluidic systems. Thanks to these kind of constructs it is possible to cultivate engineered tissues under continuous perfusion, in this way various physiological stimuli can be provided to cells, by supplying nutrients and oxygen.

In particular, the focus in our experiments is in liver cells, since they play a crucial role in drug

metabolism.

One of the main reasons for drug withdrawal is drug-induced hepatotoxicity. This is why there is need to develop robust *in vitro* model for hepatotoxicity evaluation.

Latest developments in technologies for microfabrication have made possible the fabrication of structures that are able to mimic *in vivo* conditions.

The efforts are especially focused on the development of three-dimensional models with human cells able to replicate *in vivo* cell/cell, cell/ECM (extracellular matrix) interface, moreover the tissues architecture, available for drug toxicology studies and long term functionality.

The latest methods use a well-suited matter for mimic of physical and chemical characteristics of ECM, that is the hydrogel such as gelatin. This is why cells are often encapsulated in poly(ethylene glycol) diacrylate (PEGDA).

These platforms allow the reduction in expensive reagents consumption, provide reproducibility and scalability, and allow for temporal control of drug dosage.

Moreover, one of the most desirable characteristic in tissue behaviour analysis during long-term culture period is the easy accessibility to the hepatic structure without any damage.

5.2 Bioreactor design and fabrication

Hepatocytes are responsive to the levels of oxygen concentration in the media to which they are exposed to.

COMSOL Multiphysics (COMSOL Inc.) has been used to simulate the laminar flow inside the bioreactor and to estimate the oxygen level within the cell culture chamber.

To ensure that the oxygen concentration was sufficient for cell growth, cell number has been evaluated by simulation.

The physics module used to simulate oxygen consumption on COMSOL was Transport of Diluted Species.

Oxygen is considered as a diluted rather than a concentrated species in culture media since its solubility is very low in aqueous solutions.

Oxygen consumption of cells has been evaluated through Michaelis-Menten kinetics:

$$R_{O_2} = V_{max} \frac{c_{O_2}}{c_{O_2} + K_{MM,O_2}} \delta(C_{O_2} > C_{cr})$$

where V_{max} represents the maximum volumetric oxygen consumption rate, C_{O_2} is the oxygen concentration in the cell layer, K_{MM,O_2} is the Michaelis constant equal to $6.3 \cdot 10^{-3} mol/m^3$.

$$V_{max} = \frac{qN_{cell}}{V}$$

where q is the oxygen consumption per cell ($2.2 \cdot 10^{-16} mol s^{-1}$, N_{cell} is the cell number and V is the volume of cell blocks.

Different transport properties were attributed for diluted species within the fluid and the hydrogels accordingly to different values of the diffusion coefficient. In particular, oxygen diffusion coefficient in the aqueous solution is equal to $3.8 \cdot 10^{-9} m^2 s^{-1}$, while inside the hydrogel it is equal to $0.5 \cdot 10^{-9} m^2 s^{-1}$.

The bioreactor has been entirely made by impermeable PMMA layers in order to be completely sealed from the environment atmosphere and to maintain hypoxic conditions inside the microfluidic setup of the liver-on-a-chip.

The oxygen level at the inlet was considered to be steady, uniform and equal to 13%, which is the optimal oxygen concentration in human hepatic tissue.

The design of bioreactor is shown in Figure 5.1.

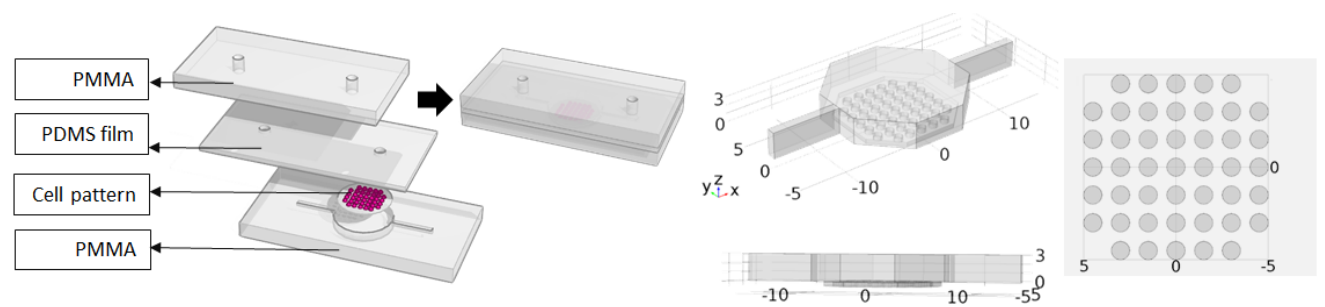


FIGURE 5.1. Schematic of liver-on-a-chip bioreactor where the patterned 3D encapsulated liver cells were entrapped within the bottom PMMA layer and covered with a top PMMA layer. An elastic PDMS membrane was sandwiched between PMMA layers for sealing. Photomask design and geometry of the bioreactor.

The dimensions and geometry of the chamber and channels have been optimized to ensure a uniform fluid flow distribution and the devices have been created using a simple and convenient process with laser ablation.

Grooves (1 mm in diameter and 0.5 mm in height) have been designed in order to entrap photo-patterned cells within GelMA blocks.

The photomask has been designed based on the simulation of required cell number within bioreactor.

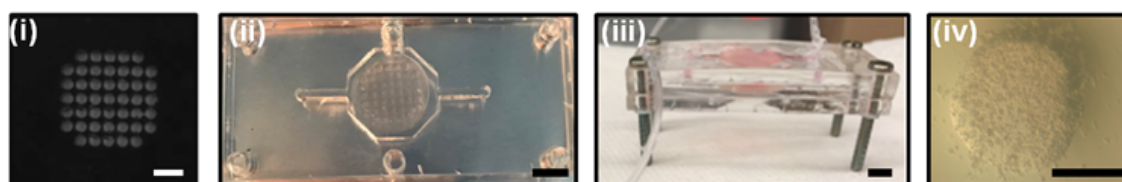


FIGURE 5.2. Photographs of (i) photomask for patterning, (ii) top view and (iii) side view of bioreactor, and a micropillar of 3D encapsulated cells.

Figure 5.3 shows the oxygen concentration gradient in the bioreactor when varying the inlet culture media flow rate from 200 to 800 $\mu L h^{-1}$.

The oxygen diffusion along the bioreactor has been simulated throughout a time-dependent study, the results show the system condition after 24 hours of culture media under perfusion flow.

The amount of dissolved oxygen inside the bioreactor dropped from the constant value at the inlet of 13% to 2% at the outlet for the slowest flow rate, while it dropped to 5% for the largest flow rate.

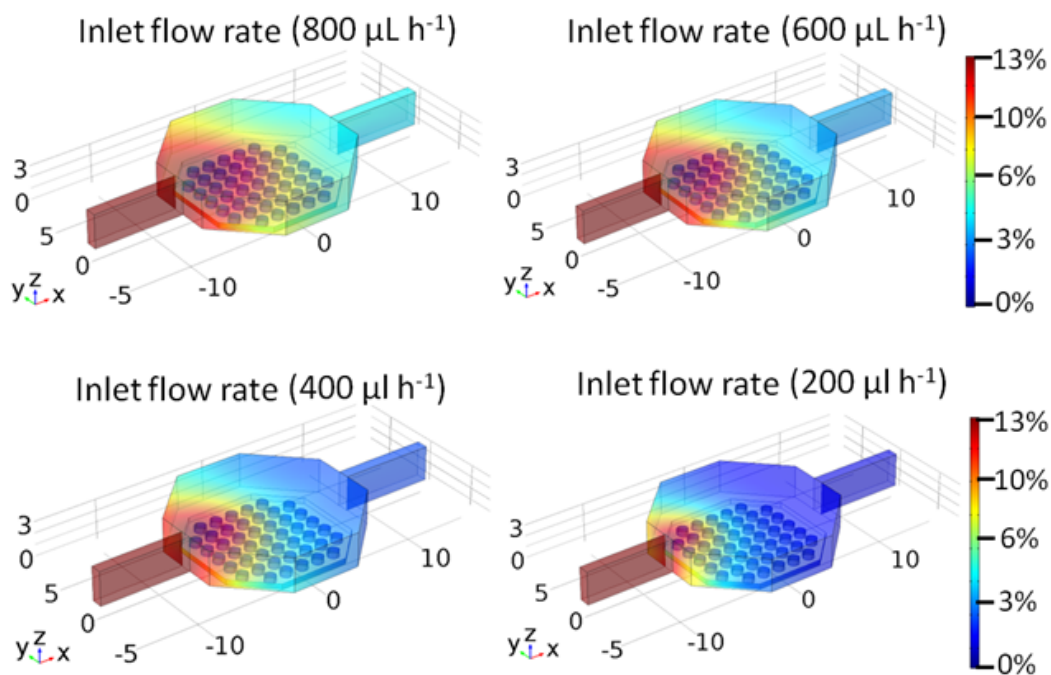


FIGURE 5.3. Oxygen uptake rate for $4 \cdot 10^6$ cells/ mL (70.000 cells in the hepatic construct) at different inlet flow rates. Scale bar = $mol m^{-3}$. Scale = 1 mm.

5.3 Oxygen effect on liver on chips

Effect of oxygen level on livers on chips has been investigated in plastic-based bioreactors.

Cultural media with oxygen level at 0%, 13% and 21% have been infused into livers on chips by using a syringe pump.

Sample was kept under $37^\circ C$ in a customized incubator.

The viability and proliferation of the 3D encapsulated cells in plastic chips have been evaluated by Live/Dead Assay test.

Live/Dead Assay is useful to differentially labels dead and live cells with fluorescent dyes.

By using a fluorescent microscopy it is possible to rapidly quantify the cell viability.

The solution used for Live and Dead assay is a mix of two different fluorescent dyes that are able to label with different colors live and dead cells: the Live cell dye labels intact, viable cells green; the Dead cell dye labels cells with compromised plasma membranes red.

A characteristic of viable cells is an intact plasma membrane and intracellular enzymatic activity.

These two features form the basis of this Live/Dead Cell Assay.

The intracellular esterase activity of live cells generates green fluorescence and excludes the red dye. On the other hand, the lack of esterase activity in dead cells and the non-intact plasma membrane allows red dye staining.

Moreover a proliferation test has been performed, resulting that cell proliferation in culture media with 13% was 8% higher than that in culture media with 0% and 21%.

Compared to cells in culture media with oxygen level at 0% and 21%, cells within 13% oxygen level showed highest cell proliferation.

Live/Dead Assay showed that after 7 days cell culture, more live cells (stained with green) could be observed in culture media with 13% while most of cells were dead in culture media with 0% oxygen level (Figure 5.4).

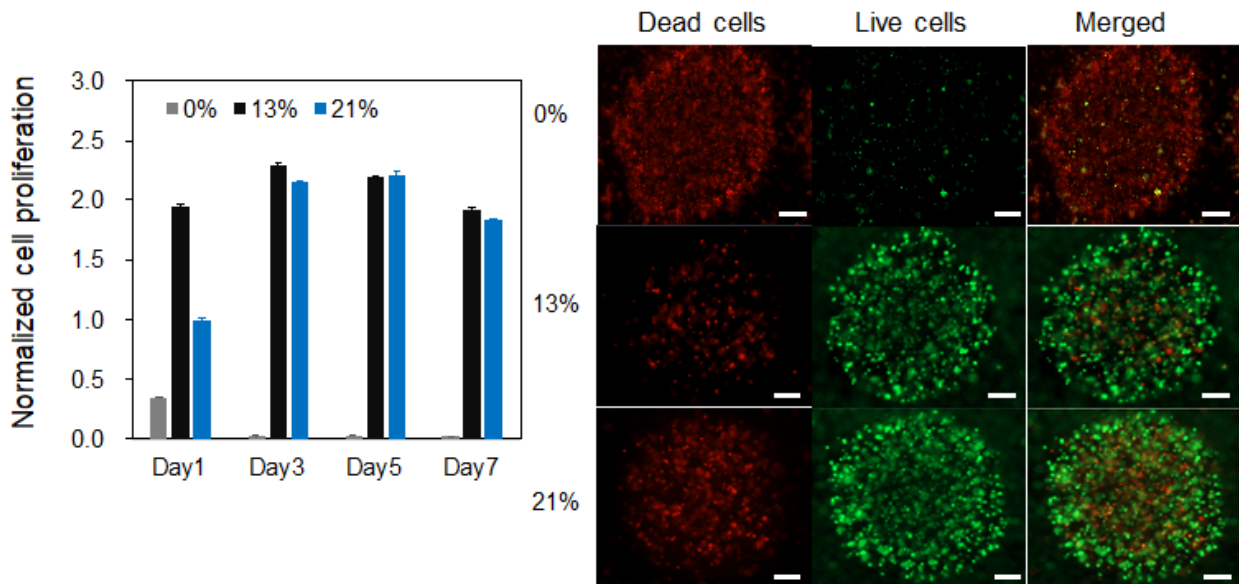


FIGURE 5.4. Cell metabolic activities as a function of different oxygen level. Scale bar= 200 μ m.

The result showed that culture media with 13% oxygen level can maintain higher viability and activity in liver on chips.

This is coherent with theoretical observations, and shows the correct behaviour of scavenger chip in providing culture media with the proper oxygen concentration.

Thanks to the developed and fabricated minimicroscope-based oxygen optical sensor previously described, the oxygen consumption of cells in day 1, 3, 5 and 7 has been analysed. The results are shown in Figure 5.5.

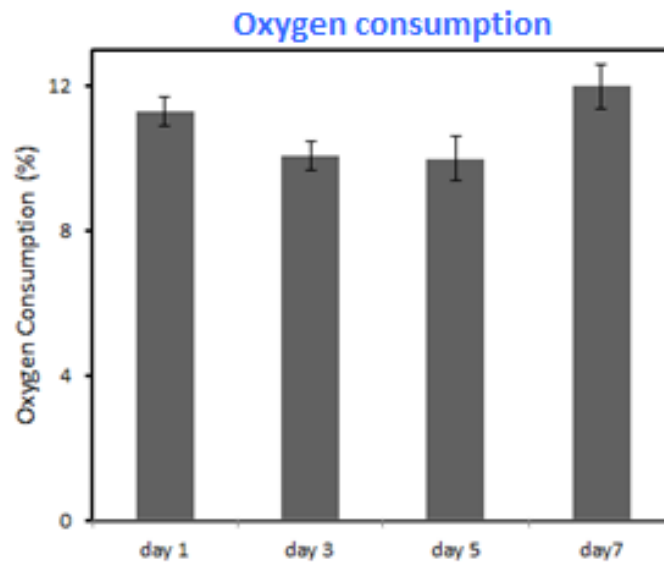


FIGURE 5.5. Oxygen consumption for 3D cell culture.

OXYGEN GENERATOR CHIP

6.1 Introduction

The oxygen *Generator chip* is designed in order to increase the oxygen concentration of culture media coming from liver on chip bioreactor.

Remembering that the aim of the project is the development of a closed-loop platform, we need to come back to the start condition after providing the bioreactor culture media with the proper oxygen concentration and verifying the cells oxygen consumption.

We started from a 21% oxygen concentration culture media (that is the typical oxygen concentration of media left in contact with air) and we decreased the oxygen concentration by using the oxygen scavenger chip to the proper level for cells in bioreactor (13%, optimal for liver cells, in this project).

At the output of the oxygen scavenger chip the culture media oxygen concentration is verified to be the correct one by using the minimicroscope-based oxygen optical sensor.

The culture media is then lead to the liver-on-chip bioreactor, where cells performed an oxygen consumption.

The culture media at the output of the liver-on-chip bioreactor is again analysed by using the minimicroscope-based oxygen optical sensor and the oxygen level results to be around 5%.

From this oxygen level, an increase is needed in order to provide culture media available for oxygen scavenging.

The oxygen generator chip has the aim of increase the culture media oxygen level from 5% to 21%.

The oxygen delivery in its most basic form is the passive diffusion from the external atmosphere through a material (characterized by gas-permeability) directly into the cell culture media.

Thanks to its gas permeability, PDMS is the material chosen with this aim.

The idea is to simply diffuse oxygen in the medium present in the system by connecting the culture media with atmosphere (with an oxygen concentration of 21%) through a very thin PDMS membrane. In this way the evaporation and contamination of media is avoided, but an oxygen gradient is still created, allowing the rapid equilibration of medium with oxygen.

This is a very simple and effective idea, allowing for a large degree of control.

6.2 Oxygen Generator chip design and fabrication

Oxygen generator has been designed and fabricated by using a patterned microchannel within PDMS matrix covered with a PDMS membrane with a thickness of $\sim 13\mu\text{m}$.

The fabrication of the microfluidics has been achieved by using a designed PMMA mold with a thickness of 3.2 mm.

The PDMS membrane has been prepared by a spinning,Àicoating method (5000 rpm for 1 min).

The PDMS matrix and PDMS membrane have been treated with plasma device for 2 min.

One of the most used matter for microfluidics fabrication is a silicone-based polymer: the polydimethylsiloxane (PDMS).

In particular, the attractive characteristics of this polymer are its low cost, elastomeric property, easy fabrication, biocompatibility and optical transparency. Beside these benefits, the hydrophobicity of PDMS is limitative in certain applications.

Chemical synthesis and analysis of biological samples often need hydrophilic surface in order to work rapidly. For this reason one largely used method in PDMS microfluidic devices fabrication

is the Oxygen plasma treatment.

The oxygen plasma treatment provides polar function groups on PDMS, like silanol group (SiOH). This lead to changes in the surface characteristics of PDMS by making it hydrophilic from hydrophobic.

Plasma treatment of PDMS increases exposes silanol groups (-OH) at the surface of the PDMS layers so that they form strong covalent bonds (Si-O-Si) when brought together with another PDMS surface. These covalent bonds form the basis of a practically inseparable seal between the layers.

The combined PDMS has been incubated at 80°C for 1 h. The prepared generator chip has been sandwiched between two PMMA sheets.

The schematic and photograph of the designed oxygen generator chip is shown in Figure 6.1. It can be observed that the coil channel is interleaved with deeper regions with arrow shapes. This let the mixing of culture media by allowing the bottom layer of media, not in contact with the PDMS membrane, to move on top and so on. Moreover these regions slow down the flux of culture media inside the channel.

More is the period of time in which the culture media is inside the oxygen generator chip, more is the available time to create an oxygen equilibrium between the culture media and the atmosphere.

In particular, with this design, the culture media flow inside the oxygen generator chip for more than 4 hours. In this way, achieving an oxygen level of 21% is ensured.

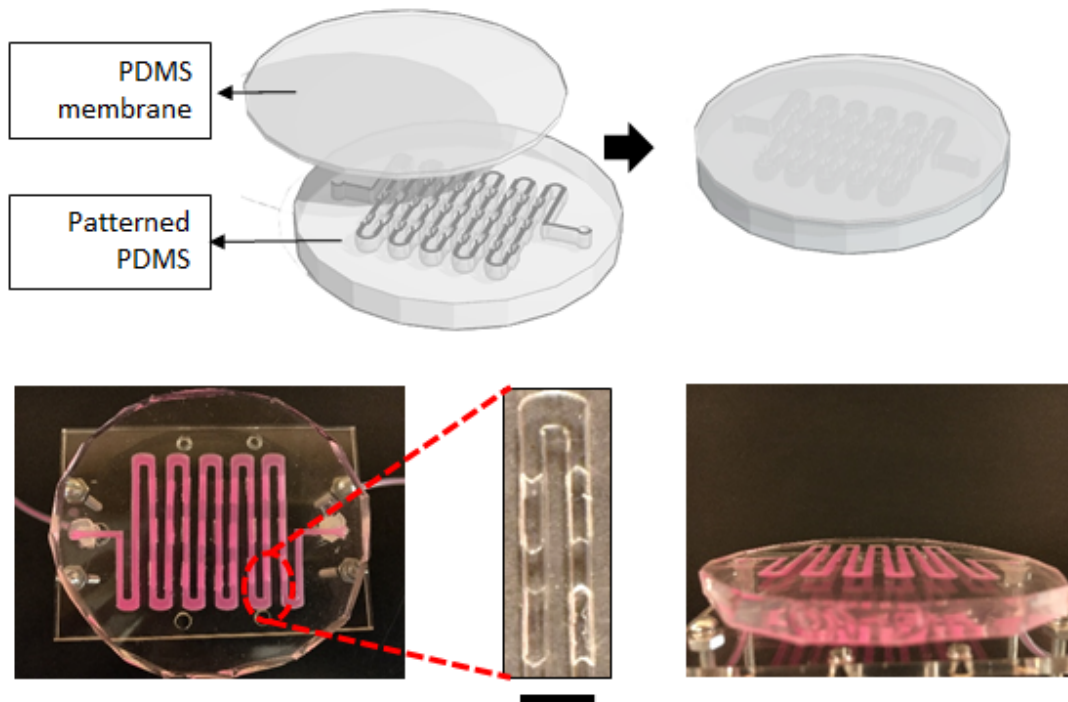


FIGURE 6.1. Schematic and photographs of oxygen generator: top view and side view. Food dye solution within the microchannels was used to demonstrate fluid flow. The magnified photograph shows a section of microfluidic patterns. Scale bar=1.5 cm. Inset scale bar=1.5 mm.

6.3 Generator test

The inlet has been connected to a syringe pump with a flow rate of $200\mu Lh^{-1}$.

The oxygen concentration of the culture medium has been measured using the minimicroscope-based optical oxygen sensor.

The cropped fluorescence image has been analysed using a MATLAB code. The result shows that the oxygen concentration increased from 5% to 21% using the oxygen generator.

The results are shown in Figure 6.2.

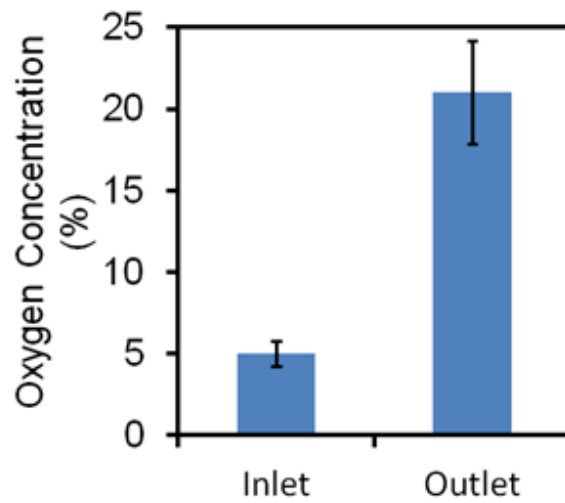


FIGURE 6.2. Measured oxygen level at both inlet and outlet.

The stability of oxygen level created by the oxygen generator chip has been tested for a time of 180 min.

The results are coherent with the expectation and are shown in Figure 6.3.

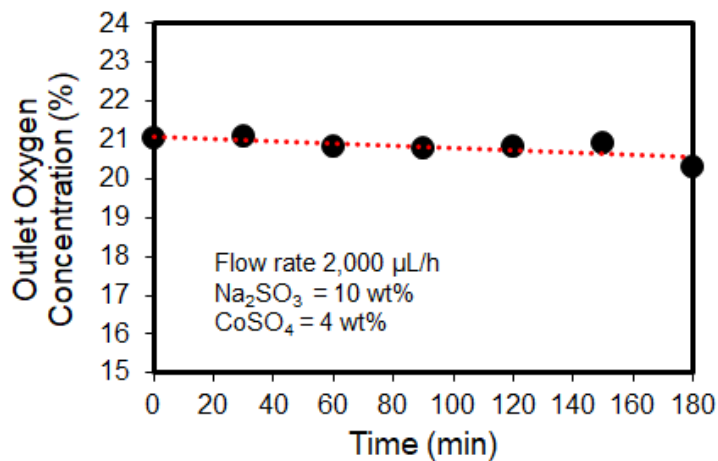


FIGURE 6.3. Stability of the oxygen generator with a prolonged time of 180 min.

7.1 Introduction

The last step of the project is the integration of the whole system. The system consists of: the oxygen scavenger chip connected to one minimicroscope-based optical oxygen sensor, this is connected to the liver-on-chip bioreactor, its the output is connected to the second minimicroscope-base optical oxygen sensor, that is connected to the oxygen generator chip.

The main channel of the system is related to the flux of cell culture media, with a flow rate of $200\mu Lh^{-1}$.

The flow rate is controlled by using a peristaltic pump.

Another flow rate needs to be controlled, that is the one of the bottom channel of the oxygen scavenger chip, dedicated to the sodium sulfite scavenging solution.

Different decreases of cell culture media oxygen concentration can be reached with the oxygen scavenger chip by varying the sodium sulfite scavenging solution flow rate. The percentage of oxygen concentration reduction increase by increasing the flow rate of the sodium sulfite scavenging solution.

The peristaltic pump that controls the sodium sulfite solution flow rate needs to be automatically

controlled.

A schematic of the whole system developed is shown in Figure 7.1.

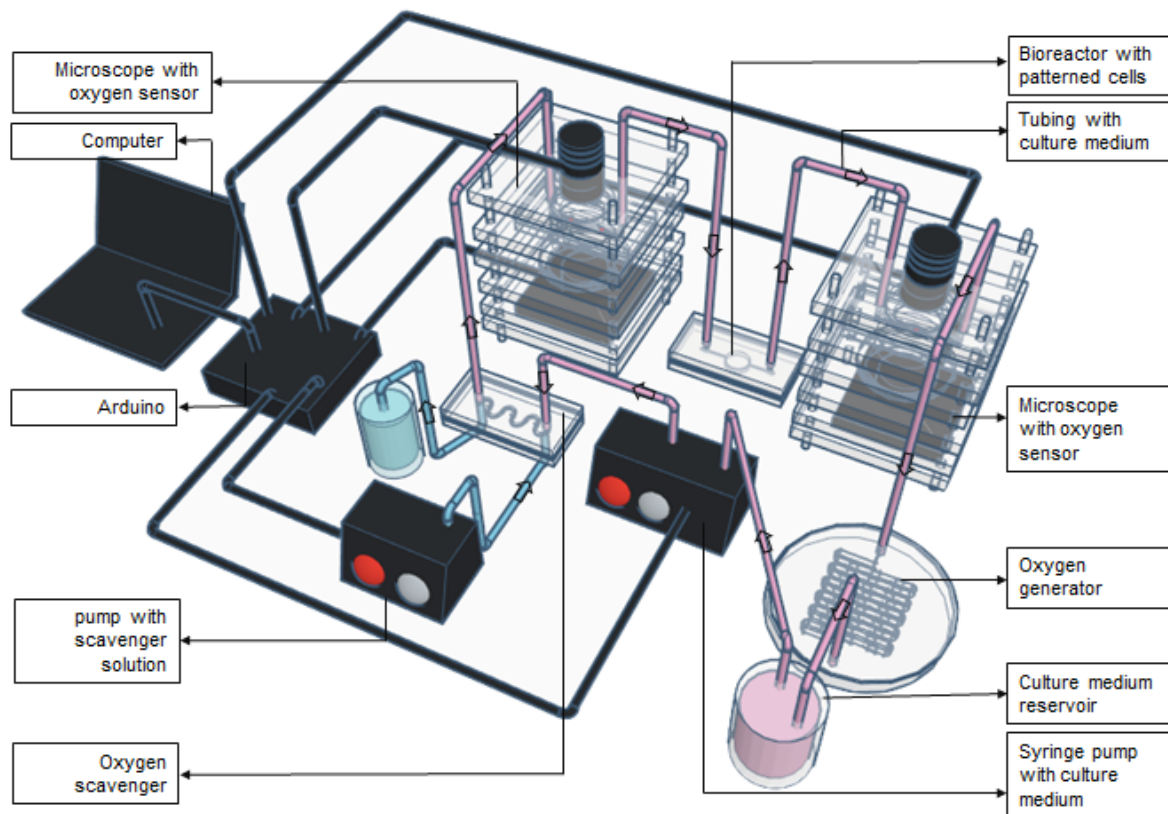


FIGURE 7.1. Layout of the Close-Loop Oxygen Control System.

An Arduino and MATLAB code have been implemented in order to control and adjust the peristaltic pump related to the sodium sulfite channel rotation speed. Moreover, an Arduino and MATLAB code have been developed in order to control the minimicroscope-based optical oxygen sensor: the camera is commanded in order to take picture at regular intervals and a T-Cube LED driver is controlled in order to properly turn on and off the LED.

7.2 Integration and control

An automatized control system has been built using electronic parts and connected to the rest of the closed-loop system.

The whole system is ultimately controlled by a custom-coded MATLAB program, which serves as the central control hub.

The computer controls an Arduino Mega 2560 microcontroller, which is connected as a master to a peristaltic pump (BQ80S Microflow Peristaltic Pump, Golander Pump) serving as a slave.

Additionally, the two blue LED470s (Thorlabs) of the mini-microscopes are wired in trigger mode to the Arduino via a BNC connector.

At the same time, the two cameras of the mini-microscopes are connected by an USB port to the laptop running MATLAB.

The control system functions by modifying the output flow rate of the peristaltic pump, which in turn changes the final concentration of oxygen in the media at the output of the scavenger chip.

The process of control is as follows. First, the MATLAB code is run, which initializes both mini-microscopes and the Arduino, which is communicated with MATLAB via a serial port.

Immediately after, the Arduino triggers both LEDs in the mini-microscopes on, and MATLAB takes 2 pictures, one for each oxygen sensor chip.

Once the pictures are taken, MATLAB sends a signal to the Arduino to turn the LEDs off. The LEDs are only switched on when taking a picture to avoid photobleaching of the sample.

MATLAB processes the pictures, targeting only the significant areas of change in the chip, and taking the average.

A classifier coded in the program decides the signal that is to be sent to the Arduino to control the pump; the behaviour of this classifier uses fuzzy logic to correlate the characterization curve of the scavenger to a physical change in the speed of the pump.

The signal is sent to the Arduino, which then stores it and sends it to the peristaltic pump.

The Arduino is connected to the Peristaltic pump using RS485 communication and a MODBUS protocol.

The connection between the Arduino and the pump is carried out by a converter (MAX485, Maxim

Integrated).

The microcontroller controls the revolutions per minute of the pump (ranging from 0.1 to 80), which in turns control the speed of the pumped media (with a range between 0.005 and 32ml/min).

The working range for the closed-loop system is between 1000 and 2000 μ l/hour.

The microcontroller can also control start/stop, and direction.

A communication-based setting of the flow has been preferred, as it is safer and allows a far more precise control (up to 0.5% deviation of the nominal flow) compared to analogue alternatives, especially considering the very low flow rates used.

7.3 Peristaltic Pump control

A peristaltic pump is a positive-displacement pump (PDP) used to pump fluids.

The pump is provided by a circular casing in which is possible to fit a flexible tube where the fluid is carried.

The fluid motion is guaranteed by a rotor, with "rollers" fixed to the external circumference of the rotor, that performs a compression on the flexible tube.

When the rotor turns, the flexible tube portion in contact with the rotor is compressed and so occluded. This forces the fluid pump and motion through the tube.

Peristaltic pumps are particularly suited for pumping sterile fluids without exposing those fluids to contamination from exposed pump components.

The peristaltic pump used in this project is the BQ80S Micro flow Variable-Speed Peristaltic Pump.

BQ80S is a portable microflow variable-speed peristaltic pump, that provides flow range from 0.005mLmin⁻¹ to 64mLmin⁻¹, compatible with the project's specifications, since a minimum flow rate of 1000 μ Lh⁻¹ is needed.

It offers basic functions such as start/stop, reversible direction and adjustable speed.

With standard RS485 MODBUS interface, it is easy to communicate with external device, such as PC with the use of Arduino.

7.4 RS485 interface

The RS485 interface supports standard MODBUS RTU protocol.

In simple terms, MODBUS is a serial communication protocol, used for information transmission between electronic devices using serial lines.

The Modbus Master is the device that requests information, while the Modbus Slaves are the devices providing information.

Pump can communicate with external device via the communication port.

The connection between the Arduino and the pump is carried out by a converter (MAX485, Maxim Integrated).

In RTU mode, the communication protocol is characterized by different fields, where the allowable characters are hexadecimal 0-9, A-F.

The start of the message is constituted by at least 3.5 character and is a silent interval.

The network bus is continuously monitored by the devices, including during the silent intervals.

After the start, the transmission continues with the device address.

After the address field transmission, the device decodes the address in order to determine if they are the addressed device.

When a device finds to be the addressed device, it decodes the whole message and acts consequently.

The devices that are not being addressed, keep monitoring for the following messages.

The message end is again characterized by the transmission of a silent interval of at least 3.5 characters.

After the end of a message, a new message can be transmitted.

The whole message is always transmitted as a continuous stream in order to be properly received.

When silent intervals of more than 1.5 characters interrupt the continuous stream before the end of the message, the incomplete message is flushed by the receiving device, that will wait for the next byte assuming that it will be a new address or message.

If a new message starts earlier than 3.5 characters after the previous one, it will be considered by the receiving device as a continuance of the previous message. This will lead to an error, since the Cyclic redundancy check will not allow combined messages.

The transmission protocol message frame described above is shown in the table (7.1).

START	ADDRESS	FUNCTION	DATA	CRC CHECK	END
T1-T2-T3-T4	8 BITS	8 BITS	n x 8 BITS	16 BITS	T1-T2-T3-T4

Table 7.1: RTU Message Frame

Address Field: The first field is the address field, containing 8 bits. The master (Arduino in our case) send the slave (the peristaltic pump) address in this field. As a result the slave sends its response by placing its own address in the first field of the response so that the master knows which slave is responding (when the master is connected to multiple slaves).

Function Field: The second field is the function field, characterised by 8 bits. In this field, the master send a function to the addressed slave, that is a code coding the action that the slave needs to perform. The slave will respond by placing in this field a code indicating a normal (error free) transmission or an error in case some kind of error occurred.

Data Field: The third field contains the data, that are transmitted in sets of 2 hexadecimal digits (from 00 to FF). In this field the master send additional information to the slave in order to be used to take the action coded in the function field. When the transmission occurs without errors, the slave responds by placing the requested data in the data field. When an error occurs, the slave send an exception code in the data field. This code is then used by the master in order to decide the next action.

CRC Error Checking: The CRC, Cyclic Redundancy Error, is an error-detecting code used to detect errors. In this field is contained the result of the CRC evaluation on the message transmitted.

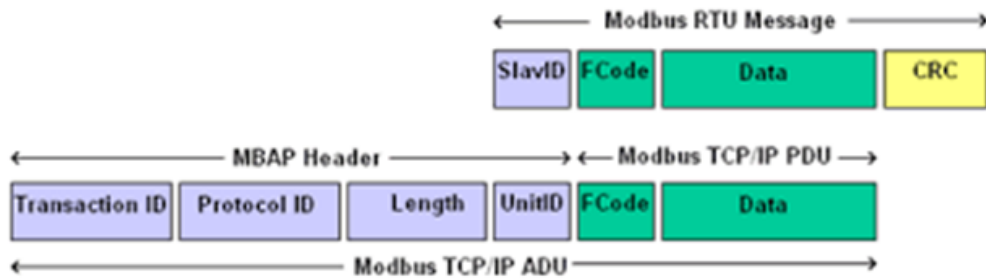


FIGURE 7.2. MODBUS protocol. The protocol consists of a series of bits, which specify the slave address, data and closure.

7.5 Connection schematic

In order to connect Arduino and the peristaltic pump, a transceiver is used.

The transceiver used is the MAX485 chip, a slew-rate-limited and low power transceiver used for RS485 communication.

It works as a single +5V power supply and the rated current is $300\mu A$.

An half-duplex communication is adopted in order to implement the function of converting TTL level of Arduino into RS485 level of the peristaltic pump.

MAX485 Connection diagram

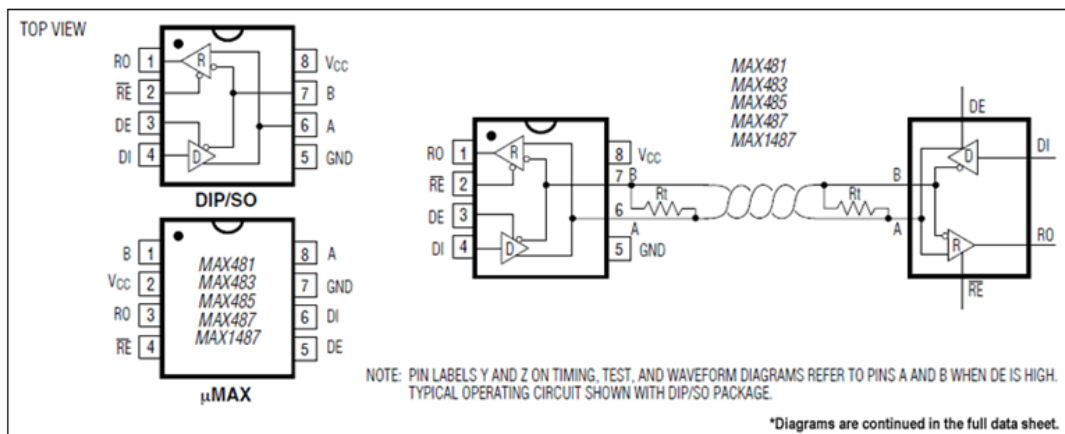


FIGURE 7.3. MAX485 connection diagram for the integrated circuit. The 4 pin on the left are connected to Arduino.

7.6 MATLAB and Arduino code for integration

After the camera initialization (basilar settings), with the *timer* function of MATLAB, the *Integration* function is called every 2 minutes.

The *Integration* function send the parameter to Arduino in order to turn on the minimicroscope LED, to take the picture from the minimicroscope, turn off the LED.

Once taken the image, it is analysed with the MATLAB function described in the Oxygen Sensor chapter.

From the value obtained with this analysis, Arduino set the rotation speed of the peristaltic pump.

Arduino set the rotation speed and turn on/turn off the peristaltic pump by writing in registers 0C1C (for rotating speed) and 0C1E (for starting/stopping the pump).

As it can be observed in the Arduino code reported below, two functions are needed prior and after transmission, with the *preTransmission()* function the driver outputs are enabled, while the receiver outputs are set as high impedance, with the *postTransmission()* function the receiver outputs are enabled while the driver outputs are set as line receivers.

The Arduino code read serial data that are sent from the MATLAB code in order to turn on, turn off the LED and set the rotation speed of the pump.

In order to set the rotation speed of the pump, Arduino write in the proper registers of the pump the value sent by the MATLAB code.

The MATLAB code send the serial value *turnon* in order to turn on the microscope LED.

Once the LED is on, the MATLAB code send the snapshot command to the microscope in order to take the image.

Once the image is taken the MATLAB code send the serial value *turnoff* to Arduino in order to turn off the microscope LED.

The image is then analysed (in the code below the analysis code is not reported since it is described in the previous chapter).

The value of the oxygen concentration obtained from the analysis is used in order to set the speed rotation of the pump.

The value is stored as *pumpval* and is send to Arduino. Below the Arduino code and MATLAB codes. Integration.ino:

```
#include <ModbusMaster.h>

int an, sn, en;
int on=0;

#define MAX485_DE      2
#define MAX485_RE_NEG  3
#define Microscope1    6
#define Microscope2    7

// instantiate ModbusMaster object
ModbusMaster node;

void preTransmission()
{
    //Driver Output Enabled, Receiver Output Disabled
    digitalWrite(MAX485_RE_NEG, 1);
    digitalWrite(MAX485_DE, 1);
}

void postTransmission()
{
    //Receiver Output Enabled, Driver Output Disabled, they functions as line receive
    digitalWrite(MAX485_RE_NEG, 0);
    digitalWrite(MAX485_DE, 0);
}
```

```
// the setup function runs once when you press reset or power the board
void setup() {
  // initialize digital pin LED_BUILTIN as an output.
  pinMode(Microscope1, OUTPUT);
  pinMode(MAX485_RE_NEG, OUTPUT);
  pinMode(MAX485_DE, OUTPUT);
  digitalWrite(MAX485_RE_NEG, 0);
  digitalWrite(MAX485_DE, 0);

  // Modbus communication runs at 9600 baud
  Serial.begin(9600);
  Serial1.begin(9600,SERIAL_8E1);

  // Modbus slave ID 1
  node.begin(1, Serial1);
  // Callbacks allow us to configure the RS485 transceiver correctly
  node.preTransmission(preTransmission);
  node.postTransmission(postTransmission);
}

bool state = true;

// the loop function runs over and over again forever
void loop() {
  uint8_t result, start;

  if (Serial.available()){
    an=Serial.read();
```

```
if (en==0){
  if (an==3){
    an=an+1;
    sn=an;
    on=1;
  }
  else if(an==7){
    an=an+1;
    sn=an;
    on=0;
  }
  else if(an==1){
    // slave: write TX buffer to (2) 16-bit registers starting at register 0
    Serial.println(2);
    en=1;
  }
  if(on==1){
    digitalWrite(Microscope1,HIGH);
    Serial.println(sn);
  }
  else{
    digitalWrite(Microscope1,LOW);
    Serial.println(sn);
  }
}
else{
  if(an!=1){
    result = node.writeSingleRegister(0x0C1C, an);
    start= node.writeSingleRegister(0x0C1E, 0x0001);
```

```
    delay(200);  
    Serial.println(9);  
    en=0;  
  }  
}  
}
```

MATLAB: Initialize.m:

```
%%Mini Microscope 1  
clear cam  
delete(instrfindall)  
arduino=serial('COM4','BaudRate',9600);  
fopen(arduino);  
cam=webcam('KAV_HD_MF_2MP');  
cam.Brightness=50;  
cam.Saturation=30;  
cam.Contrast=30;  
cam.WhiteBalanceMode='manual';  
cam.WhiteBalance=4000;  
cam.ExposureMode='auto';  
cam.Hue=0;  
cam.Gamma=100;  
cam.BacklightCompensation=1;  
preview(cam)
```

MATLAB: TimerIntegration.m:

```
Initialize  
a=timer;  
set(a,'ExecutionMode','fixedRate')
```

```
set(a, 'TasksToExecute', Inf)  
set(a, 'Period', 120)  
set(a, 'TimerFcn', @(~,~) Integration(cam, arduino));  
set(a, 'StopFcn', @(~,~) Finish(arduino));  
start(a);
```

MATALB: Integration.m:

```
function [meanvalue, snap]=Integration(cam, arduino)  
  
turnon=3;  
turnoff=7;  
pumpsw=1;  
i=0;  
j=0;  
k=0;  
while i==0  
    fwrite(arduino, turnon, 'char');  
    dt=fscanf(arduino, '%f', 1);  
    if dt==4  
        i=1;  
    end  
end  
pause(2);  
snap=snapshot(cam);  
while i==1  
    fwrite(arduino, turnoff, 'char');  
    dt=fscanf(arduino, '%f', 1);  
    if dt==8  
        i=0;  
    end
```

```
end

%%Processing
snap=snap(:, :, 1);
%%Copy-Paste image processing code
meanvalue=mean(mean(snap))*10; %Mean Value of CHip after processing
evalin('caller', ['clear_', 'meanvalue'])
evalin('caller', ['clear_', 'snap'])
assignin('base', 'meanvalue', meanvalue);
assignin('base', 'snap', snap);
%%Scavenger part and function
%%
%%Classifier
if meanvalue<=10
    pumpval=34;
else
    pumpval=100;
end
while j==0
    fwrite(arduino, pumpsw, 'char');
    dt=fscanf(arduino, '%f', 1);
    if dt==2
        while k==0
            fwrite(arduino, pumpval, 'char');
            wt=fscanf(arduino, '%f', 1);
            if wt==9
                k=1;
            end
        end
    end
    j=1;
```

end

end

end

MATALB: FinishIntegration.m:

closePreview(cam)

fclose(arduino);

delete(instrfindall)

stop(a)

delete(a)

clear all

CONCLUSIONS

Here, an automated closed-loop liver on chip system is created, that provides dynamic and continuous oxygen control and monitoring.

The multiplex liver on chip platform features in four aspects: an automated oxygen monitoring system; oxygen scavenger composed of two engraved microchannels and an embedded PDMS membrane for decreasing oxygen level; an oxygen generator for increasing oxygen level and a liver on chip platform containing a peristaltic pump, a bioreactor and fresh cultural media. To create this multiplexing oxygen controlled livers on chips, all of the microfluidics chips have been made from laser patterned poly(methyl methacrylate) (PMMA) layers and sealed by thermal treatment.

The automated livers on chips have been programmed by a computer and operated in an automated manner for at least 7 days.

The geometry and performance of each microfluidic chip have been investigated separately, including mini-microscope-based oxygen optical sensor, oxygen scavenger, oxygen generator and bioreactor.

The automation control system has been tested and analyzed.

Oxygen level has been achieved in real-time monitoring and dynamically adjusted to adapt to liver-on-a-chip model system.

Long-term drug responses and short-term evaluation of acute toxicity under different oxygen levels to the mimicked liver tissues have been assessed within the closed loop system.

The on-chip circulation has been driven by a peristaltic pump with a flow rate of $200\mu Lh^{-1}$ and has been powered by a programmed MATLAB code.

This code has been also written to drive the LED controllers for monitoring oxygen level in the system at predetermined time points and controlling the syringe pump integrated with oxygen scavenger.

The closed-loop liver-on-a-chip platform has been designed to be modular, including a programmable controlling system for microfluidic routing and oxygen level regulation and real-time monitoring, microbioreactors for housing liver organoids, two customized mini-microscope integrated with oxygen optical sensors, bilayered oxygen scavenger connected to a syringe pump, and oxygen generator for oxygen exchange.

Individual modules have been interconnected by using Teflon tubes which allow for fluid flow in the circulation.

To achieve real-time monitoring of oxygen level within the system, a microfluidic oxygen sensor was integrated with a customized mini-microscope where fluorescence intensity of the sensing microbeads has been observed and converted to the dissolved oxygen concentration in the programmed software.

Several tests have been performed and one of the results is that the correctness of the mini-microscope based optical oxygen sensor has been verified. The measurement of oxygen concentration in culture media is possible with an optical sensor with a proper accuracy in order to monitor culture media oxygen level.

Moreover, the correctness of oxygen scavenger chip and oxygen generator chip have been tested. The result is that it is possible to control the oxygen percentage of the cell culture media by decreasing it without the risk of leading to culture media toxicity. The chip used guarantees the creation of an oxygen gradient with no physical contact between the scavenging solution and the cell culture media. Moreover has been verified the possibility to control the amount of oxygen percentage decrease by varying the flow rate of the scavenging solution, providing a robust and sufficiently accurate characteristic curve.

The oxygen generator chip capability has been tested so that a closed loop system can be used by increasing and decreasing the cell culture media oxygen level in the several sections of the loop. The whole system has been automatized and tested by letting it work for seven days. The possibility of an automatized closed loop system able to monitor in real time and continuously the percentage of oxygen present in the cell culture media has been verified.

BIBLIOGRAPHY

- [1] Y. S. Zhang, J. Ribas, A. Nadhman, J. Aleman, S. Selimovifá, S. C. Lesher-Perez, T. Wang, V. Manoharan, S. Shin, A. Damilano, N. Annabi, M. R. Dokmeci, S. Takayama and Ali Khademhosseini, *A cost-effective fluorescence mini-microscope for biomedical applications*, Lab on a Chip, 2015, 15, 3661.
- [2] M. D. Brennan, M. L. Rexius-Hall, D. T. Eddington, *A 3D-Printed Oxygen Control Insert for a 24-Well Plate*, PLOS ONE, Arum Han, Texas AM University, UNITED STATES, 2015.
- [3] C. Peng, W. Liao, Y. Chen, C. Wu and Y. Tung, *A microfluidic cell culture array with various oxygen tensions*, Lab on a Chip, 2013, 13, 3239.
- [4] Y. Li¹, L. Li¹, Z. Liu¹, M. Ding¹, G. Luo¹, Q. Liang¹, *A microfluidic chip of multiple,Ächannel array with various oxygen tensions for drug screening*, Microfluid Nanofluid, Springer-Verlag Berlin Heidelberg 2016.
- [5] S. Halldorsson, E. Lucumi, R- Gomez-Sjoberg, R. M.T. Fleming, *Advantages and challenges of microfluidic cell culture in polydimethylsiloxane devices*, Biosensors and Bioelectronics 63, 2015, 218-231.
- [6] A. P. Vollmer, R.d F. Probststein, R. Gilbert and T. Thorsen, *Development of an integrated microfluidic platform for dynamic oxygen sensing and delivery in a flowing medium*, Lab Chip, 2005, 5, 1059,Ä1066.
- [7] P. E. Oomen, M. D. Skolimowski and E. Verpoorte, *Implementing oxygen control in chip-based cell and tissue culture systems*, Lab Chip, 2016, 16, 3394.

- [8] M. L. Shuler, *Organ-, body- and disease-on-a-chip systems*, Lab Chip, 2017, DOI: 10.1039/c7lc90068f.
- [9] A. D. Stroock, S. K. W. Dertinger, A. Ajdari, I. Mezic, H. A. Stone, G. M. Whitesides, *Chaotic Mixer for Microchannels*, SCIENCE VOL 295, 2002.
- [10] L. Wang, W. Liu, Y. Wang, J. Wang, Q. Tu, R. Liub and J. Wang, *Construction of oxygen and chemical concentration gradients in a single microfluidic device for studying tumor cell-drug interactions in a dynamic hypoxia microenvironment*, Lab Chip, 2013, 13, 695.
- [11] D. B. Papkovsky and R. I. Dmitriev, *Biological detection by optical oxygen sensing*, Chem. Soc. Rev., 2013, 42, 8700.
- [12] S. G. Charati and S. A. Stern, *Diffusion of Gases in Silicone Polymers: Molecular Dynamics Simulations*, Macromolecules 1998, 31, 5529-5535.
- [13] T. C. MERKEL, V. I. BONDAR, K. NAGAI, B. D. FREEMAN, I. PINNAU, *Gas Sorption, Diffusion, and Permeation in Poly(dimethylsiloxane)*, Journal of Polymer Science: Part B: Polymer Physics, Vol. 38, 415-434 (2000).
- [14] Y. Chen, A. D. King, H. Shih, C. Peng, C. Wu, W. Liao and Y. Tung, *Generation of oxygen gradients in microfluidic devices for cell culture using spatially confined chemical reactions*, Lab Chip, 2011, 11, 3626.
- [15] J. M. Vanderkooi, G. Maniara, T. Green, and D. F. Wilson, *An Optical Method for Measurement of Dioxygen Concentration Based upon Quenching of Phosphorescence*, THE JOURNAL OF BIOLOGICAL CHEMISTRY, Vol. 262, No. 12, pp. 5476-5482, 1987.
- [16] H. KAUTSKY, *QUENCHING OF LUMINESCENCE BY OXYGEN*, German, 1938.
- [17] GR. LIEBSCH, I. KLIMANT, B. FRANK, G. HOLST, and O. S. WOLFBEIS, *Luminescence Lifetime Imaging of Oxygen, pH, and Carbon* Society for Applied Spectroscopy, Volume 54, Number 4, 2000.

BIBLIOGRAPHY

- [18] N. S. Bhise, V. Manoharan, S. Massa, A. Tamayol, M. Ghaderi, M. Miscuglio, Q. Lang, Y. S. Zhang, S. R. Shin, G. Calzone, N. Annabi, T. D. Shupe, C. E. Bishop, A. Atala, M. R. Dokmeci and Ali Khademhosseini, *A liver-on-a-chip platform with bioprinted hepatic spheroids* *Biofabrication* 8 (2016) 014101.
- [19] S. M. Borisov and I. Klimant, *Luminescent nanobeads for optical sensing and imaging of dissolved oxygen* Springer-Verlag 2008.
- [20] M. B. Byrne, M. T. Leslie, H. R. Gaskins, and P. J.A. Kenis, *Methods to study the tumor microenvironment under controlled oxygen conditions* *Trends in Biotechnology* November 2014, Vol. 32, No. 11.
- [21] M. Skolimowski, M. W. Nielsen, Je. Emneus, S. Molin, R. Taboryski, C. Sternberg, M. Dufva and O. Geschkes, *Microfluidic dissolved oxygen gradient generator biochip as a useful tool in bacterial biofilm studies* *Lab Chip*, 2010, 10, 2162,Äi2169.
- [22] B. Ungerbock, V. Charwat, P. Ertl and T. Mayr, *Microfluidic oxygen imaging using integrated optical sensor layers and a color camera* *Lab Chip*, 2013, 13, 1593.
- [23] W. Yang, C. Luo, L. Lai, and Q. Ouyang, *A novel microfluidic platform for studying mammalian cell chemotaxis in different oxygen environments under zero-flow conditions* *BIOMICROFLUIDICS* 9, 044121 (2015).
- [24] H. Shiku, T. Saito, C. Wu, T. Yasukawa, M. Yokoo, H. Abe, T. Matsue, and H. Yamada, *MOxygen Permeability of Surface-modified Poly(dimethylsiloxane) Characterized by Scanning Electrochemical Microscopy* *Chemistry Letters* Vol.35, No.2 (2006).
- [25] M. A. Omary and H. H. Patterson, *Luminescence, Theory* *Encyclopedia of Spectroscopy and Spectrometry*, Third Edition, 2017.
- [26] S. M. Grist, L. Chrostowski and K. C. Cheung, *Optical Oxygen Sensors for Applications in Microfluidic Cell Culture* *Sensors* 2010, 10, 9286-9316.

- [27] J. Ehgartner, M. Strobl, J. M. Bolivar, D. Rabl, M. Rothbauer, P. Ertl, S. M. Borisov, and T. Mayr, *Simultaneous Determination of Oxygen and pH Inside Microfluidic Analytical Chemistry* 2016, 88, 9796,â9804.
- [28] M. D. Brennan, M. L. Rexius-Hall, L. J. Elgass and D. T. Eddington, *Oxygen control with microfluidics* Lab Chip, 2014, 14, 4305.
- [29] G. Mehta, K. Mehta, D. Sud, J. W. Song, T. Bersano-Begey, N. Futai, Y. S. Heo, M. Mycek, J. J. Linderman, S. Takayama, *Quantitative measurement and control of oxygen levels in microfluidic poly(dimethylsiloxane) bioreactors during cell culture* Biomed Microdevices (2007) 9:123,â134.
- [30] K. K. Tung, R.T. Bonnecaze, B.D. Freeman, D.R. Paul, *Characterization of the oxygen scavenging capacity and kinetics of SBS films* Polymer 53 (2012) 4211-4221.
- [31] D. Sud, G. Mehta, K. Mehta, J. Linderman, S. Takayama, and Mary-Ann Mycek, *Optical imaging in microfluidic bioreactors enables oxygen monitoring for continuous cell culture* Journal of Biomedical Optics, Vol. 11(5), 2006.
- [32] P. C. Thomas, S. R. Raghavan and S. P. Forry, *Regulating Oxygen Levels in a Microfluidic Device* Analytical Chemistry 2011, 83, 8821,â8824.
- [33] S. A. M. Shaegh, A. Pourmand, M. Nabavinia, H. Avci, A. Tamayol, P. Mostafalu, H. B. Ghavifekr, Esmail N. Aghdam, M. R. Dokmeci, A. Khademhosseini, Y. S. Zhang, *Rapid Prototyping of Whole-Thermoplastic Microfluidics with Built-in Microvalves* Lab Chip, 2016, 00, 1-7.